Translational Stroke Research (2020) 11:1117–1136
https://doi.org/10.1007/s12975-020-00792-2

ORIGINAL ARTICLE

Methylprednisolone Reduces Persistent Post-ischemic Inflammation in a Rat Hypoxia-Ischemia Model of Perinatal Stroke

Svetlana Altamentova[1] · Prakasham Rumajogee[1] · James Hong[1,2] · Stephanie R. Beldick[1,2] · Sei Joon Park[1] · Albert Yee[1] · Michael G. Fehlings[1,2,3,4]

Received: 15 August 2019 / Revised: 12 January 2020 / Accepted: 19 February 2020 / Published online: 5 March 2020

Abstract

In perinatal stroke, the initial injury results in a chronic inflammatory response caused by the release of proinflammatory cytokines, gliosis and microglia activation. This chronic and ongoing inflammatory response exacerbates the brain injury, often resulting in encephalopathy and cerebral palsy (CP). Using a neonatal rat model of hypoxia-ischemia (HI) at postnatal day (P)7, we demonstrated that chronic inflammation is persistent and continues into the tertiary phase of perinatal stroke and can be attenuated by the administration of methylprednisolone sodium-succinate (MPSS, 30 mg/kg), a US Food and Drug Administration (FDA) approved anti-inflammatory agent. The inflammatory response was assessed by real-time quantitative PCR and ELISA for markers of inflammation (CCL3, CCL5, IL18 and TNFα). Structural changes were evaluated by histology (LFB/H&E), while cellular changes were assessed by Iba-1, ED1, GFAP, NeuN, Olig2 and CC1 immunostaining. Functional deficits were assessed with the Cylinder test and Ladder Rung Walking test. MPSS was injected 14 days after HI insult to attenuate chronic inflammation. In neonatal conditions such as CP, P21 is a clinically relevant time-point in rodents, corresponding developmentally to a 2-year-old human. Administration of MPSS resulted in reduced structural damage (corpus callosum, cortex, hippocampus, striatum), gliosis and reactive microglia and partial restoration of the oligodendrocyte population. Furthermore, significant behavioural recovery was observed. In conclusion, we demonstrated that administration of MPSS during the tertiary phase of perinatal stroke results in attenuation of the chronic inflammatory response, leading to pathophysiological and functional recovery. This work validates the high clinical impact of MPSS to treat neonatal conditions linked to chronic inflammation.

Keywords Perinatal stroke · Hypoxia-ischemia model · Methylprednisolone · Chronic inflammation

Introduction

Perinatal stroke is a devastating condition, with patients experiencing life-long afflictions including intellectual and physical disability, developmental and behavioural disorders [1–3], as well as an increased risk of cerebral palsy (CP) [4]. Perinatal stroke occurs between the end of the second trimester (around 22 weeks) and the first month of life affecting 1 in 4000 term births. The probability of perinatal stroke is highest in the week surrounding birth and occurs at a rate three-times higher than stroke observed in an "at-risk" adult [5]. Mechanistically, venous or arterial thrombo-embolization leads to a decrease in oxygen delivery to the brain, resulting in a host of pathophysiologic processes that cause brain damage [6, 7].

Perinatal stroke injury has been described using a "triphasic hypothesis" of brain damage, divided into acute, secondary

Svetlana Altamentova and Prakasham Rumajogee contributed equally to this work.

Electronic supplementary material The online version of this article (https://doi.org/10.1007/s12975-020-00792-2) contains supplementary material, which is available to authorized users.

✉ Michael G. Fehlings
michael.fehlings@uhn.ca

[1] Division of Genetics and Development, Krembil Research Institute, University Health Network, Toronto, Ontario, Canada

[2] Institute of Medical Science, University of Toronto, Toronto, Ontario, Canada

[3] Division of Neurosurgery, University of Toronto, Toronto, Ontario, Canada

[4] Division of Neurosurgery, Toronto Western Hospital, University Health Network, 399 Bathurst St. Suite 4WW-449, Toronto, Ontario M5T 2S8, Canada

and tertiary phases of injury [8, 9]. The acute phase occurs minutes after the initial insult, triggering cell death, activating gliosis and microglia, releasing proinflammatory cytokines and perpetuating inflammation [8–12]. The secondary phase lasts hours to days and initiates additional mechanisms such as microglial and astroglial activation, glutamate excitotoxicity, oxidative stress and alterations in neuronal signalling [8, 9, 13–16]. Finally, the tertiary phase can last for months or years and involves chronic microglial and astroglial activation (i.e. chronic inflammation), impaired oligodendrocyte development, compromised proliferation and synaptogenesis and epigenetic changes [8, 13, 17]. This chronic inflammation can exacerbate brain lesions long after the original insult [8, 9].

Perinatal stroke can lead to encephalopathy [18], elevated levels of IL-1, IL-6, IL-8, TNFα as well as increased glial fibrillary acidic protein (GFAP) in the serum of newborns that have been linked to abnormal neurological outcomes [19]. In animal models of perinatal hypoxic-ischemic (HI) injury, inflammatory processes have been shown to damage neurons and oligodendrocytes [8, 12, 20]. Activation of microglia/macrophages, CD4 lymphocytes and astroglia continues for at least 42 days after an HI insult, suggesting that HI injury leads to chronic inflammation [21]. IL18 also plays an essential role in the pathophysiology of neonatal HI, as its expression is elevated up to 14 days post-injury, while in mice lacking IL18, the mitigation of brain injury is observed [22, 23]. Therefore, targeting the inflammatory response after perinatal stroke during the tertiary phase represents a promising approach for directly impacting the extent of brain damage and reducing neurological impairment.

In animal models of perinatal stroke, glucocorticoids have been administered within hours of injury to modulate the acute inflammatory response [24–26]. In the central nervous system (CNS), glucocorticoids act by lowering levels of pro-inflammatory cytokines, attenuating reactive gliosis and infiltration of immune cells, and reducing neuronal apoptosis [27–29]. Methylprednisolone (MPSS) is a US Food and Drug Administration (FDA)–approved glucocorticoid used as an immunosuppressive agent to treat several conditions, including systemic lupus erythematosus, spinal cord injuries and multiple sclerosis, among many others [30–33]. MPSS acts through the inhibition of lipid peroxidation and has more lipid antioxidant activity than other steriods used in the clinic, for example dexamethasone [34]. In animal studies, a 30-mg/kg IV dose of MPSS administered at 5 min, 2 h and 4 h in adult rats with spinal cord injury led to reductions in tissue loss and reduced dieback of vestibulospinal fibres [35]. In a neonatal rat model, when MPSS (30 mg/kg) was injected intra-peritoneally along with vitamin E (100 mg/kg) immediately after HI injury, the ipsilateral hemisphere had significantly less water content 72 h post-HI, while significantly less damage was observed 21 days post-injury [24]. Interestingly, it has recently been reported that high-dose intravenous MPSS administration led to complete recovery in a 11-month-old child with subacute stroke [36]. However, there has been little research investigating the utility of delayed MPSS administration on attenuating chronic inflammation and subsequent brain injury.

Diagnosis of neurologic disability is frequently made late in early childhood. For example, CP is usually diagnosed around the age of two, when children fail to meet developmental milestones [37, 38]. Due to the difficulties diagnosing injury early in a child's life, we adapted a protocol for MPSS treatment in a rat neonatal HI model to target tertiary phase perinatal stroke. Animals were treated with MPSS at postnatal day (P)21, which corresponds approximately to the brain development of a 2-year-old child [39]. We hypothesized that MPSS would act as an anti-inflammatory agent to attenuate chronic inflammation in the brain following perinatal stroke, resulting in neuroprotective effects at structural and cellular levels, and lead to significant improvements in neuromotor function. To assess this hypothesis, we induced HI injury in P7 rats and used delayed MPSS treatment (P21-P22). We evaluated the impact of MPSS on the expression of pro-inflammatory markers (RT-qPCR and ELISA), brain structures and cellular changes (by histology and immunohistochemistry), as well as motor function (by neurobehavioral testing).

Materials and Methods

Study Design

We adapted the hypoxia-ischemia (HI) Rice-Vannucci model [40] to be performed on P7 rats (Fig. 1a). The infarct volume was assessed using 2,3,5-triphenyltetrazolium chloride (TTC) staining at P8, P14 and P21. After methylprednisolone sodium-succinate (MPSS) treatment (P21-P22), a subset of animals was sacrificed at P24 and markers of inflammation were evaluated. In the remaining animals, behavioural testing was done weekly from P20 to P56, until sacrifice. The brains were harvested and processed for histology and immunohistochemistry (Fig. 1b). We investigated structural, cellular and functional changes after HI, with or without MPSS treatment.

Animal Use

Experimental procedures, animal use and care were approved by the Animal Care Committee at the University Health Network in accordance with the policies and procedures outlined by the Canadian Council of Animal Care. Long Evans rats were housed under controlled conditions (12-h light/dark cycles, + 24 °C temperature and fed ad libitum with automatic watering). The day of birth was defined as postnatal day (P)0. Pups were weaned at P21.

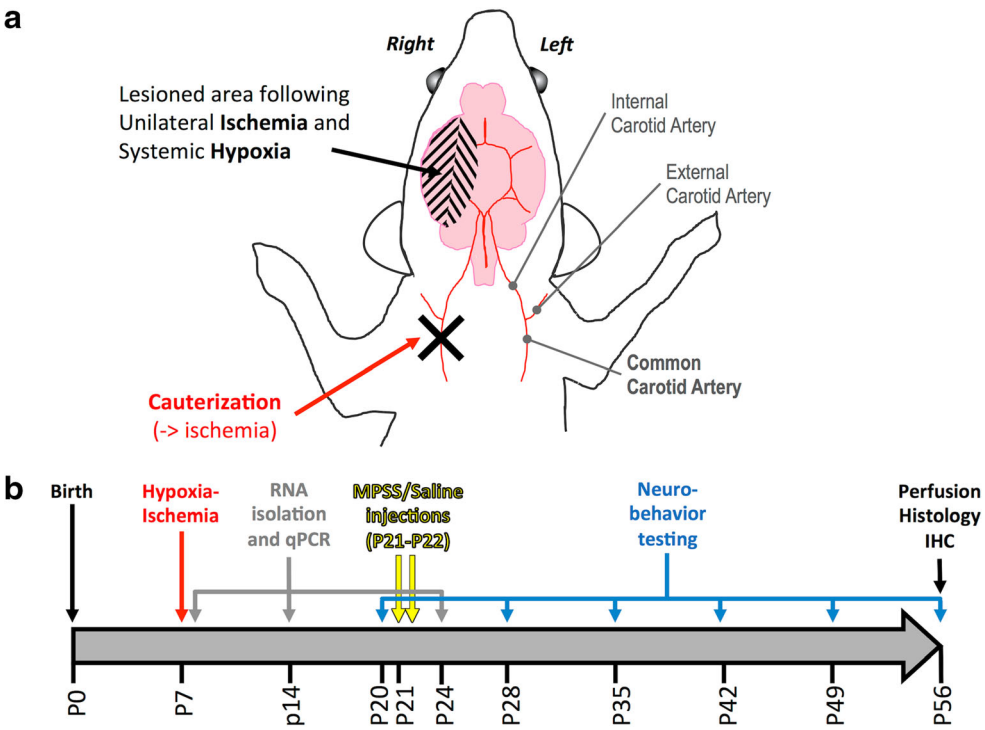

Fig. 1 Experimental design and timeline. **a** Design of the Rice-Vannucci hypoxia-ischemia (HI) model; diagram adapted with permission from Rumajogee et al. (eNeuro, 2018). **b** Timeline of the experimental procedures

HI Injury Model

To model the perinatal HI injury we used the Rice-Vannucci model [40]. In this model, the combination of right carotid artery occlusion (ischemia) and systemic hypoxia leads to unilateral brain lesions ipsilateral to the carotid occlusion (Fig. 1a), while the contralateral side remains uninjured and therefore can be considered as a control side [41]. Control rats received sham surgery (no carotid occlusion) and were not subjected to hypoxia. The HI procedure is described in our previous publication [42], with the following specific details: P7 Long Evans rats, surgical procedure 5–6 min, isoflurane exposure time adjusted to 8 min, 60 min recovery with the dam before hypoxia (75 min of 8% oxygen) and 36.5 °C water.

Although this procedure was standardized and produced reliable results, there is inherent variability with this model. Occasionally, severe lesions occurred that resulted in the destruction of brain structures. Due to the prevalence of destroyed structures in the brains of severely injured rats, we focussed on "mild/medium" injury levels while "severely" injured brains were not included in the analysis.

MPSS Injections

The sodium succinate form of methylprednisolone (MPSS) from Pfizer Canada Inc. was used due to its higher water solubility and ability to dissolve well in saline solution. We selected our MPSS dose based on previous MPSS injection protocols [43–45]. In previous animal studies, the MPSS dose used has been variable: 3 doses of 30 mg/kg [46] to 3 doses of 100 mg/kg [29], with an optimal dose of 30 mg/kg being proposed by Braughler et al. for spinal cord injury [47, 48]. Further studies have also utilized 30 mg/kg [34, 45, 46, 49, 50]; as such, we decided to use 3 intravenous injections (8 a.m. and 2 p.m. at P21, and 8 a.m. at P22) of 30 mg/kg of MPSS into the tail vein. Control animals received saline solution (0.9% NaCl). We chose P21 as the chronic time-point for treatment as it corresponds to a 2-year-old child from a developmental perspective [39], an age when neurodevelopmental disease, such as CP, is often diagnosed.

Real-Time Polymerase Chain Reaction Quantification of Gene Expression

RT-qPCR was used to assess inflammation markers, i.e. CCL3 (MIP-1α), CCL5 (RANTES), IL18 and TNFα in brain areas ipsilateral (right) and contralateral (left) to carotid occlusion. To collect brain tissue for RNA and protein analysis, rat pups were perfused with cold sterile PBS and decapitated. Brain samples were extracted and placed in cold PBS. Brain samples from the right and left hemispheres of rat pups at 1, 7 and 17 days post-injury (i.e. P8, P14 and P24) were collected, snap frozen in liquid nitrogen, and stored at − 80 °C for RNA analysis. Total RNA from each individual sample was extracted using E.Z.N.A. RNA kit (OMEGA Bio-tek, cat#R6834-01, Norcross, GA). RNA purity and quantity were assessed with a 2000C NanoDrop. Complementary DNA (cDNA) synthesis was performed using the Sensi FAST cDNA Synthesis Kit (Bioline, cat#BIO-65053, Memphis, TN). Real-time qPCR

was performed using Taqman design primers with SensiFast Probe HI-Rox Mix (Bioline, cat#82029) in a 7900HT Fast Real-Time PCR system (Applied Biosystems, Foster City, CA, http://www.appliedbiosystems.com). Supplementary Table 1 lists the Applied Biosystems Inc. (Hercules, CA) TaqMan probes used in this study. Relative quantification of gene expression was performed using the $2^{-\Delta\Delta CT}$ method that normalized the brain tissue of naive animals to an endogenous control, which was cyclophilin A (peptidylprolyl Isomerase A, PPIA). This method is described in our previous publication [51]. The number of rats used (*n*) was as follows: Naïve (5), Sham (6 for P8, P14 and P24), HI (6 for P8, P14 and P24), Sham + MPSS (6 for P24) and HI + MPSS (13 for P24).

ELISA

Brain tissue homogenates from the right (ipsilateral to injury) hemisphere were prepared as follows: frozen tissue was homogenised on ice in RIPA buffer (Thermo Scientific, cat#89901) with Halt Protease and Phosphatase Inhibitor Cocktail (Thermo Scientific, cat#78440), followed by 3 rounds of 10 s sonication. The homogenates were centrifuged at 14,000 rpm for 20 min, and the supernatants were collected for analysis. The protein was quantified with MicroBCA Protein assay (Thermo Scientific, cat#23235, MA, USA) using known concentrations of bovine serum albumin for standard curve. A total of 200 μg of protein for each sample was sent to Eve Technologies (Calgary, AB, Canada) for high throughput Luminex profiling using the rat discovery assay for cytokines/chemokines (RD27). The concentration of cytokines/chemokines was calculated using a standard curve and expressed in picograms per millilitre. A total of 20 rats were used for this assay with $n = 5$ for 4 groups.

TTC Staining

We used TTC (2%) staining to estimate the brain injury after the HI procedure. After decapitation, we used sterile razor blades and brain matrix (Ted Pella inc., cat#15052) to produce 2-mm coronal sections that were then stained using TTC according to a previously described technique [52] at P8, P14 and P21. As TTC is a potential substrate for mitochondrial cellular dehydrogenases, in healthy tissue, it is reduced to formazan, which is a deep red water-insoluble dye. Therefore, this protocol stains the uninjured tissue in red, while the injured/dead tissues will retain its original colour. The brain sections were placed in a multiplate, covered with 2% TTC solution and incubated at 37 °C for 20 min. Brain sections were scanned using a HP Scanjet G4050. The number of rats used (*n*) was as follows: 5, 6 and 5 for P8, P14 and P21, respectively, for sham and HI rats.

Tissue Processing, Histology and Immunohistochemistry

Animals were perfused at P56 to characterize the HI injury and to estimate the extent of recovery after MPSS treatment. Rodent brains were prepared for histology and immunohistochemistry, as described previously [42, 53, 54]. The brains were sectioned from the level of the genu of the corpus callosum (CC) to the splenium of the CC, as previously described [55].

Histology

Luxol fast blue (LFB) as well as hematoxylin and eosin (H&E) staining was performed according to a previously described protocol [56]. Analysis was done on a Zeiss Epifluorescence microscope with motorized platform, using the Cavalieri estimator of the Stereo Investigator software (MBF Bioscience, Williston, VT) to measure areas and distances. Number of rats used (*n*=) was as follows: 6 Sham, 7 Sham + MPSS, 10 HI and 11 HI + MPSS.

Immunohistochemistry

We performed immunostaining using commercially available antibodies and appropriate secondary antibodies. Cell type–specific markers were used: NeuN (neurons), GFAP (astrocytes), Iba-1 (microglia), ED1 (activated microglia), Olig2 (oligodendrocytes) and CC1 (astrocytes/mature oligodendrocytes). Details of primary and secondary antibodies are listed in Supplementary Tables 2 and 3. The procedure is described in our previous publication [42]. For the whole brain slice images, the slides were scanned using a Zeiss AxioScan slide scanner (20X, NA0.8 objective). Fluorescence was generated with an X-Cite 120 LED mini (Lumen Dynamics) and imaged with a Flash 4.0 sCMOS (Hamamatsu). Exposure times ranged from 50 to 200 ms. Shading correction was performed in Zeiss Zen Blue software. We also analyzed slides using a Nikon C2 laser scanning confocal microscope (20×). Images were acquired as Z-stacks for each region assessed: cortex (M1, S1), corpus callosum, hippocampus (CA1, CA3), striatum (CPu) and thalamus. The Z-stacks were combined as maximum intensity projections before analysis. Similar to histopathological analyses, all regions were assessed as a ratio (right/left). A minimum of 6 slides (3 around Bregma 0 and 3 around Bregma − 4.0) were evaluated for each animal. Researchers performing quantification were blinded to the identity of the tissue. The number of rats used (*n*) was as follows: 6 Sham, 7 Sham + MPSS, 10 HI and 11 HI + MPSS injections.

Image Analysis

Images were converted from their native Nikon format (.nd2) to 8-bit multi-channel .tiffs using the Bio-Formats reading plugin in Fiji (https://www.nature.com/articles/nmeth.2019). The images were then Z-projected using the native "Z Project" function (Max Intensity) and split using the "Split Channels" function into their respective red, green and blue channels. For all counts (CC1, Olig2, Iba-1, ED1, NeuN), images were taken through a two-step background removal procedure. First, the images were processed using the "Gaussian Blur" function ($\sigma = 3$) and then multiplied onto their respective originals using the native "Image Calculator" function for the first step of background subtraction. Second, images were taken through a rolling background subtraction using the "Subtract Background" function (rolling = 40). To improve cell count accuracy, the "Median blur" function (radius = 2) was used to smooth focal staining in cells. Finally, the cells were counted using the "Find Maxima" function (noise = 2). For CC1 and Olig2 colocalization, the "and" expression within the "Image Calculator" function was used between the CC1 and Olig2 channels to determine the colocalized pixels, with percentage of Olig2 with overlapping CC1 being the final value calculated. For GFAP staining area fraction, images were first thresholded and a size filtration using the native "Analyze Particles" function (50–500 pixels, circularity = 0) was used to exclude any edge artefacts. Images taken in the CC and pyramidal cells within the hippocampus were manually delineated through the DAPI channel for evaluation of cell counts and area fraction of staining using the "ROI manager" function.

Behavioural Testing

Functional deficits were assessed with the Cylinder and Ladder Rung Walking behavioural tests. The Cylinder test is a rearing test that assesses locomotor asymmetry and demonstrates a preference for one forelimb over another [42]. A rat is put in a clear plastic cylinder, and its rearing activity is video recorded for 5 min. The placement of the whole palm on the wall (cylinder) indicates the use of that forelimb for body support. The use of the right (R, unaffected) versus left (L, affected) forelimb is calculated as a percentage of total contacts: $R/(R + L) \times 100$.

The Ladder Rung walking test is used to assess skilled walking for both fore- and hindlimb placing, stepping and inter-limb coordination [57]. The apparatus consists of a horizontal ladder which an animal walks across. The spacing of the ladder rungs can be varied to prevent animals compensating for impairments through learning the spacing and location of the rungs. Rats were placed on the Ladder Rung and 3 runs were video recorded and then analyzed in slow motion. The number of errors and the number of total steps were counted. Total number of foot faults per forelimb were scored for each run and averaged. The success rate of the test was calculated by dividing the amount of errors to the number of total steps and presented as % foot fault rate. The number of rats (n) used for both behavioural tests was as follows: 6 Sham, 7 Sham + MPSS, 10 HI and 11 HI + MPSS injections.

Statistical Analysis

Data were processed in Excel 2016 (Microsoft). Descriptive statistics (means ± standard error of the mean (SEM); n variable per group) were calculated using GraphPad Prism (version 6.01, GraphPad Software, San Diego, CA). For histology and immunohistochemistry quantifications, multiple group comparisons were performed using a 1-way ANOVA followed by Bonferroni post-hoc test using GraphPad Prism. ELISA data was checked for Gaussian distribution and passed the Kolmogorov-Smirnov normality test and subsequently analyzed by 1-way ANOVA using GraphPad Prism. For qPCR and behavioural analysis, multiple group comparisons were performed using a 2-way ANOVA followed by Bonferroni post-hoc using GraphPad Prism. Values reported are mean ± SEM. Exact p values are reported. n.s. = not significant; $*p < 0.05$, $**p < 0.01$, and $***p < 0.001$.

Results

Inflammation in the Ipsilateral Brain Hemisphere Persists After Perinatal Stroke

We first confirmed the presence of chronic brain lesions induced by perinatal stroke using TTC staining at P8 (1 day), P14 (1 week) and P21 (2 weeks post insult) (Fig. 2a). The white/pink areas reveal dead tissue, which was observed mostly in the cortex, hippocampus, CC and striatum of the ipsilateral/injured hemisphere. The contralateral hemisphere remained red, indicating healthy and uninjured areas, and therefore represents the "control" side of the brain in our hemiplegic model. We then investigated the inflammation state using real-time qPCR (Fig. 2b). Our results show that the expression of pro-inflammatory cytokines (i.e. CCL3, CCL5, IL18, and TNFα) was persistently upregulated in the lesioned brain tissue.

The expression level of CCL3 (Fig. 2b/i) was increased 24 h after HI (P8) in the ipsilateral/injured hemisphere of the HI brain (24.65 ± 3.82), compared to the contralateral/uninjured hemisphere (7.97 ± 0.62, $p = 0.278$) or to the ipsilateral hemisphere of the Sham rat brain (2.63 ± 0.19, $p = 0.014$). This significant increase persisted at P14 in the ipsilateral HI hemisphere (24.72 ± 12.6) compared to its contralateral counterpart (1.66 ± 0.37, $p = 0.008$) and to the ipsilateral hemisphere of the Sham brain (1.07 ±

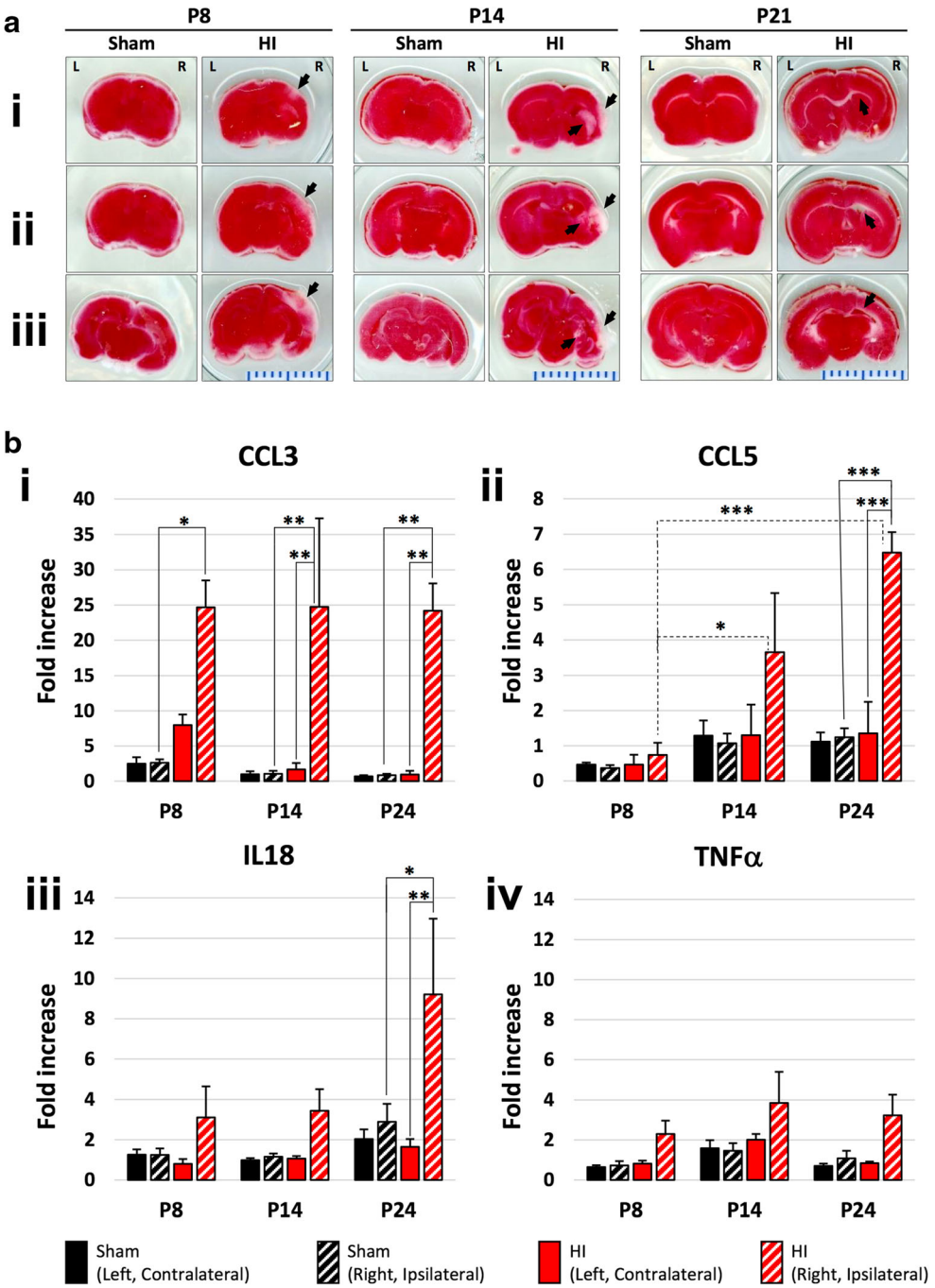

Fig. 2 Evolution of the brain injury after hypoxia-ischemia. **a** TTC staining showing HI injury in the rat brain (at P8, P14, P21). TTC staining of 3 brain level sections (rostro-caudally i, ii and iii) of P8 ($n = 6$), P14 ($n = 5$) and P21 ($n = 5$) HI and Sham animals. Dead tissue is visualised in white or pink colour. Arrows point to lesioned areas (e.g. cortex, striatum, corpus callosum, hippocampus). L left/control side; R right/injured side; scale marks are millimetres. **b** RT-qPCR results show persistent inflammation after HI at P8, P14 and P24. Gene expression of inflammatory markers CCL3 (i), CCL5 (ii), IL18 (iii) and TNFα (iv) in the contralateral/left (plain bars) and ipsilateral/right (dashed bars) brain areas of Sham rats (black bars) and HI rats (red bars) at 1 day (P8), 7 days (P14) and 17 days (P24) after HI. Number of rats used (n=): 6 for P8, P14 and P24 for each group. Values reported are mean ± SEM; $^{*}p < 0.05$, $^{**}p < 0.01$ and $^{***}p < 0.001$

0.17, $p = 0.005$). Similarly, at P24 CCL3 expression remained elevated in the ipsilateral HI hemisphere (24.17 ± 3.90), compared to the contralateral hemisphere (0.94 ± 0.007, $p = 0.007$) and to the ipsilateral hemisphere of Sham brain (0.85 ± 0.08, $p = 0.006$).

The CCL5 expression level after HI (Fig. 2b/ii) did not increase at P8. However, it increased at P14 and P24, reaching statistical significance at the late time-point. At P24, CCL5 expression reached 6.48 ± 0.58 in the ipsilateral HI hemisphere, compared to 1.35 ± 0.37 ($p < 0.001$) in the contralateral hemisphere or to 1.24 ± 0.25 ($p < 0.001$) in the ipsilateral hemisphere of the Sham rat brain. Interestingly, CCL5 expression was significantly upregulated at P14 (3.66 ± 1.68) and P24 (6.48 ± 0.58) in the ipsilateral hemisphere of HI brain compared to P8 (0.74 ± 0.35, $p = 0.042$ and $p < 0.001$, respectively).

The IL18 expression level after HI (Fig. 2b/iii) slightly increased at P8 and P14. Interestingly, it reached significance later at P24: 9.21 ± 3.75 (ipsilateral HI hemisphere) versus 1.64 ± 0.38 (contralateral HI hemisphere, $p = 0.005$).

The expression levels of TNFα after HI (Fig. 2b/iv) also increased at P8, P14 and P24 but did not reach significance.

In summary, we showed an upregulation of CCL3, CCL5 and IL18 in the ipsilateral hemisphere of the HI brain at P8, with the significant increases persisting (P14 and P24).

Delayed MPSS Administration Attenuates Chronic Inflammation Following Perinatal Stroke

We assessed the RNA and protein expression levels of inflammatory markers (i.e. CCL3, CCL5, IL18 and TNFα) after MPSS treatment (P21–22) at the chronic time-point P24 (Fig. 3). No differences were observed between Sham and Sham + MPSS groups for any of the markers investigated (statistical data not shown). The mRNA level of CCL3 (Fig. 3a/i) increased significantly after injury (24.17 ± 3.90) compared to Sham animals (0.85 ± 0.08, $p < 0.001$). After treatment, a significant restoration was observed (9.95 ± 3.67, $p = 0.002$). Figure 3a/ii shows that CCL5 mRNA expression significantly increased after HI (6.48 ± 0.58, versus Sham 1.24 ± 0.25, $p < 0.001$) and significantly decreased after treatment (3.80 ± 0.63, $p = 0.006$). Similarly, IL18 mRNA levels significantly increased after HI (9.21 ± 3.75, versus Sham 2.89 ± 0.89, $p = 0.012$) and were restored to 2.16 ± 0.41 ($p = 0.004$) after treatment (Fig. 3a/iii). However, Fig. 3a/iv shows only a tendency for TNFα to increase after HI (3.23 ± 1.03 versus Sham 1.08 ± 0.38, $p = 0.054$), which is restored after treatment (1.50 ± 0.23, $p = 0.059$).

The expression of pro-inflammatory cytokines was verified for protein content using ELISA (Fig. 3b). As no differences in mRNA were observed in the left/uninjured hemisphere between groups, we estimated the protein content of cytokines/chemokines in the right/injured hemisphere only. Similar to the level of mRNA, the level of CCL3 protein increased significantly after HI injury (Fig. 3b/i) at P24 (17.20 ± 5.54 pg/ml) compared to Sham animals (1.19 ± 0.25 pg/ml, $p = 0.008$). After MPSS treatment, it was partially restored (5.34 ± 1.97 pg/ml). The level of CCL5 protein also increased significantly (Fig. 3b/ii) (4.45 ± 0.64 pg/ml, $p = 0.04$) compared to Sham animals (2.89 ± 0.15 pg/ml) and showed a tendency to decrease after treatment (3.74 ± 0.45 pg/ml). Figure 3b/iii shows that the level of IL18 protein significantly increased after HI (449.61 ± 73.35 pg/ml, $p = 0.0018$) compared to Sham animals (182.10 ± 6.78 pg/ml) and decreased significantly after treatment (241.30 ± 36.54 pg/ml, $p = 0.015$). Figure 3b/iv shows only a slight increase in TNFα protein after HI (0.45 ± 0.14 pg/ml), which was restored after treatment (0.24 ± 0.08 pg/ml).

We demonstrated that at P24 for both RNA and protein, the levels of CCL3, CCL5, IL18 and TNFα (though not significantly) were elevated after HI and that expression of these inflammatory markers was partially restored following MPSS treatment.

Delayed MPSS Administration Attenuates Chronic Histopathological Structural Changes Following Perinatal Stroke

We analyzed brain structural outcomes at P56 (Fig. 4; Supplemental Fig. 1). This late time point leaves enough time for the treatment to have an impact on brain structures and neurobehavioral performance. Representative images of brain coronal sections at bregma levels around 0 and − 4.0 mm (Fig. 4a) show that the lesions are observed in the right/ipsilateral side in several major brain structures (e.g. cortex, CC, hippocampus, ventricle, striatum, thalamus), at anterior and posterior levels. The injury is partially restored in MPSS-treated rats. MPSS did not have an impact on control animals (Sham versus Sham + MPSS).

After HI injury, the brain size changed, with the right injured hemisphere being significantly smaller (0.66 ± 0.03) compared to the contralateral uninjured hemisphere or to the sham ipsilateral hemisphere (1.01 ± 0.02, $p < 0.001$) (Fig. 4b/i). After MPSS treatment, the size of the right hemisphere of injured animals was partially restored (0.82 ± 0.02) compared to injured animals without treatment (0.66 ± 0.03, $p < 0.001$) but still remained smaller compared to sham animals (1.01 ± 0.02, $p < 0.001$).

The right ventricle (Fig. 4b/ii) area increased significantly after HI (3.65 ± 1.03) compared to sham animals (1.02 ± 0.11, $p < 0.01$). Following MPSS treatment, the size of the ventricle was partially restored (1.88 ± 0.36) compared to untreated animals (3.65 ± 1.03, $p < 0.05$) but was not statistically larger compared to sham animals (1.02 ± 0.11, $p = 0.590$).

The ipsilateral motor cortex (M1; Fig. 4b/iii) was thinner (0.85 ± 0.02) in the injured animals compared to ipsilateral M1 of sham animals (1.03 ± 0.03, $p < 0.001$) and was restored after MPSS treatment (1.02 ± 0.01, $p < 0.001$). The somatosensory cortex (S1) of the ipsilateral brain hemisphere of HI rats (S1, Fig. 4b/iv) was thinner (0.82 ± 0.02) compared to S1 of sham rats (1.00 ± 0.03, $p = 0.004$). After MPSS treatment, recovery was observed (0.97 ± 0.03, $p = 0.004$). The difference between HI + MPSS and Sham rats was not significant for both M1 and S1, showing almost full recovery.

The area of the right CC (Fig. 4b/v) decreased after HI (0.70 ± 0.02) compared to the sham animals (1.04 ± 0.03, $p = 0.002$). After treatment, the right area of CC increased (0.92 ± 0.08) compared to the untreated injured animals (0.70 ± 0.02, $p = 0.028$) and was not significantly different from the right area of CC in sham animals (1.04 ± 0.03, $p = 0.433$). We did not observe significant changes in the thickness of CC (Fig. 4b/vi).

We observed a dramatically smaller right hippocampus (0.57 ± 0.03) in the ipsilateral HI brain compared to the uninjured contralateral hemisphere or to the ipsilateral hemisphere of sham rats (1.01 ± 0.04, $p < 0.001$) (Fig. 4b/vii). After MPSS treatment, the ipsilateral hippocampus size slightly increased

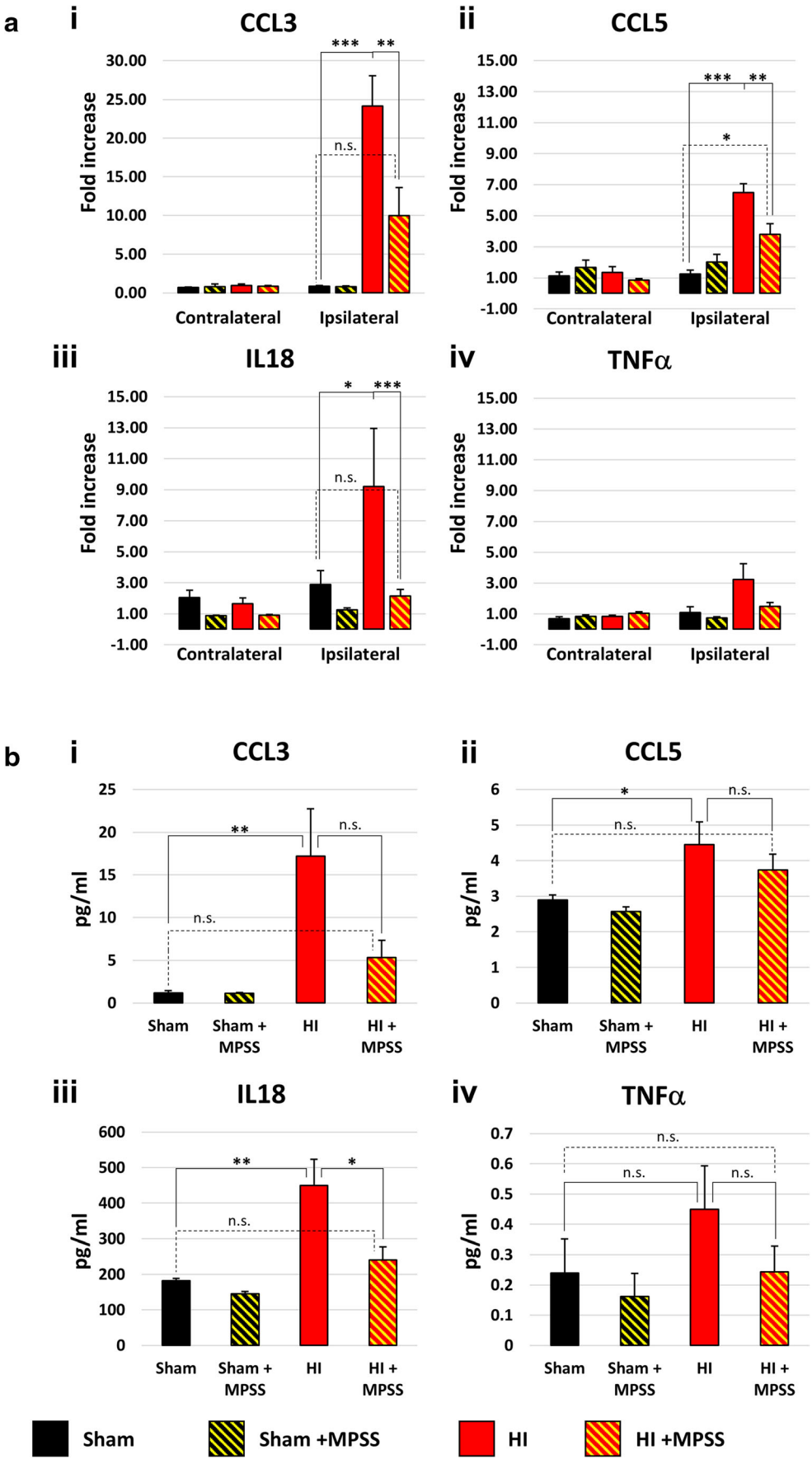
a
i
CCL3
Fold increase
30.00
25.00
20.00
15.00
10.00
5.00
0.00
***
**
n.s.
Contralateral
Ipsilateral
ii
CCL5
Fold increase
15.00
13.00
11.00
9.00
7.00
5.00
3.00
1.00
-1.00
***
**
*
Contralateral
Ipsilateral
iii
IL18
Fold increase
15.00
13.00
11.00
9.00
7.00
5.00
3.00
1.00
-1.00
*
***
n.s.
Contralateral
Ipsilateral
iv
TNFα
Fold increase
15.00
13.00
11.00
9.00
7.00
5.00
3.00
1.00
-1.00
Contralateral
Ipsilateral
b
i
CCL3
pg/ml
25
20
15
10
5
0
**
n.s.
n.s.
Sham
Sham + MPSS
HI
HI + MPSS
ii
CCL5
pg/ml
6
5
4
3
2
1
0
*
n.s.
n.s.
Sham
Sham + MPSS
HI
HI + MPSS
iii
IL18
pg/ml
600
500
400
300
200
100
0
**
*
n.s.
Sham
Sham + MPSS
HI
HI + MPSS
iv
TNFα
pg/ml
0.7
0.6
0.5
0.4
0.3
0.2
0.1
0
n.s.
n.s.
n.s.
Sham
Sham + MPSS
HI
HI + MPSS
Sham
Sham +MPSS
HI
HI +MPSS

◀ **Fig. 3** Administration of MPSS (at P21–22) attenuates chronic inflammation. **a** Gene expression of inflammatory markers CCL3 (i), CCL5 (ii), IL18 (iii) and TNFα (iv) in the contralateral/left and ipsilateral/right brain areas of control rats (Sham, black bars) and HI rats (red bars) without MPSS treatment (plain bars) or with MPSS treatment (yellow-dashed bars), administered at P21–22. Following HI, all four inflammatory markers are increased in the injured ipsilateral brain area when compared to the uninjured contralateral control area or the uninjured ipsilateral brain area of the sham animal. After MPSS treatment, we observed a significant decrease in inflammatory markers, which was significant for CCL3, CCL5 and IL18, compared to untreated HI animals. Number of rats used (n=): 13 for HI + MPSS, 6 for other groups. Values reported are mean ± SEM. n.s. = not significant; *$p < 0.05$, **$p < 0.01$ and ***$p < 0.001$. **b** Protein expression of inflammatory markers CCL3 (i), CCL5 (ii), IL18 (iii) and TNFα (iv) in the ipsilateral/right brain areas of control rats (Sham, black bars) and HI rats (red bars) without MPSS treatment (plain bars) or with MPSS treatment (yellow-dashed bars), administered at P21–22. Following HI, all four inflammatory markers are increased in the injured ipsilateral brain area, when compared to the uninjured contralateral control area or the uninjured ipsilateral brain area of the sham animal. After MPSS treatment, we observed smaller increases to these markers as compared to untreated HI animals. Number of rats used ($n = 5$) for each group. Values reported are mean ± SEM. n.s. = not significant; *$p < 0.05$, **$p < 0.01$

(0.66 ± 0.03) compared to untreated HI animals (0.57 ± 0.03, $p = 0.152$) but remained much smaller than sham animals (1.01 ± 0.04, $p < 0.001$).

Delayed MPSS Treatment Improved Microglial, Astroglial and Oligodendrocyte Populations but Only Partially Restored Neuronal Populations

Delayed MPSS Treatment Partially Restores Iba-1 and ED1-Positive Microglia Populations

Investigating the changes at a cellular level, we analyzed the presence of microglia using Iba-1 and ED1 (CD68) markers, known as markers of inflammation (Figs. 5 and 6). Iba-1 immunoreactivity significantly increased following HI in the ipsilateral CC (2.60 ± 0.23) (Fig. 5a/ii) and hippocampus areas (CA1 2.09 ± 0.14 and CA3 1.61 ± 0.07) (Fig. 6a/ii and iii) compared to sham animals (CC 1.06 ± 0.08, $p < 0.001$; CA1 1.01 ± 0.11, $p < 0.001$; CA3 0.99 ± 0.10, $p = 0.001$). After MPSS treatment, Iba-1 decreased in the ipsilateral CC (1.75 ± 0.09) (Fig. 5b/i) and in the hippocampus areas (CA1 1.47 ± 0.09, and CA3 1.13 ± 0.101) (Fig. 6b/i and iii), compared to untreated HI animals (CC 2.60 ± 0.23, $p = 0.002$; CA1 2.09 ± 0.14, $p = 0.006$; CA3 1.61 ± 0.07, $p = 0.011$). After treatment, no differences were observed with sham animals (CC: $p = 0.082$; CA1: $p = 0.277$; CA3: $p = 0.855$). ED1 immunoreactivity also significantly increased after HI in the ipsilateral CC (6.27 ± 0.57) (Fig. 5a/ii) and hippocampus areas (CA1 6.72 ± 0.64 and CA3 3.47 ± 0.31) (Fig. 6a/ii and iii) compared to sham animals (CC 0.85 ± 0.21, $p = 0.042$; CA1 1.33 ± 0.29, $p < 0.001$; CA3 0.85 ± 0.13, $p < 0.001$). After MPSS treatment, ED1 level was partially restored in the ipsilateral CC (2.24 ± 0.55) (Fig. 5b/ii) and hippocampus areas (CA1 3.82 ± 0.75 and CA3 1.55 ± 0.35) (Fig. 6b/ii and iv) of injured animals compared to untreated HI animals (CC 6.27 ± 0.57, $p = 0.001$; CA1 6.72 ± 0.64, $p = 0.004$; CA3 3.47 ± 0.31, $p = 0.002$). After treatment, no differences were observed with sham animals (CC: $p = 0.820$; CA1: $p = 0.214$; CA3: $p = 0.607$).

Delayed MPSS Treatment Attenuates Gliosis

We investigated gliosis in the sensorimotor cortex, caudoputamen (CPu), hippocampus and thalamus after HI (Figs. 7 and 8). GFAP immunoreactivity (Figs. 7 and 8) slightly increased after HI in the cortex areas (M1 1.81 ± 0.38; S1 3.48 ± 1.00) (Fig. 7a/ii and iv) when compared to sham animals (M1 1.02 ± 0.17, $p = 0.105$; S1 0.99 ± 0.14, $p < 0.05$). After treatment, GFAP levels decreased (M1 1.36 ± 0.12; S1 1.87 ± 0.31) when compared to untreated injured HI animals (M1 1.81 ± 0.38, $p = 0.406$; S1 3.48 ± 1.00, $p = 0.151$) (Fig. 7b/i and ii). In the CPu (Fig. 7a/iii), GFAP immunoreactivity significantly increased after HI (5.20 ± 0.80) when compared to control animals (0.86 ± 0.05, $p < 0.001$) and was restored after MPSS treatment (1.80 ± 0.43) when compared to untreated HI animals (5.20 ± 0.80, $p < 0.001$) (Fig. 7b/iii). There were no significant differences between treated and control animals (M1: $p = 0.701$; S1: $p = 0.822$; CPu: $p = 0.808$). In the hippocampus (Fig. 8a/ii and iii), GFAP immunoreactivity increased significantly (CA1 2.00 ± 0.26 and CA3 2.09 ± 0.11) when compared to control animals (CA1 0.92 ± 0.11, $p = 0.005$ and CA3 0.97 ± 0.13, $p < 0.001$). Following treatment, GFAP levels were reduced (CA1 1.28 ± 0.15; CA3 1.48 ± 0.16) when compared to injured animals (CA1 2.00 ± 0.26, $p = 0.078$; CA3 2.09 ± 0.11, $p = 0.011$) (Fig. 8b/i and ii). In the thalamus (Fig. 8a/iv), GFAP immunoreactivity significantly increased after HI (2.09 ± 0.27) compared to sham animals (1.13 ± 0.07, $p = 0.027$) and was restored after treatment (1.25 ± 0.14, $p = 0.018$) (Fig. 8b/iii).

Delayed MPSS Treatment Has a Limited Effect on the Neuronal Population

The neuronal population was slightly reduced after HI injury, with the number of NeuN-positive cells being smaller in the ipsilateral hemisphere of the brain (Figs. 7 and 8). We found a significant decrease of NeuN-positive cells in the ipsilateral CA1 area (Fig. 8a/ii and c/i) of the injured hemisphere (0.71 ± 0.04) compared to sham animals (0.97 ± 0.09, $p = 0.008$). After MPSS treatment, NeuN-positive cells were restored (0.95 ± 0.03) when compared to untreated HI animals (0.71 ± 0.04, $p = 0.003$) (Fig. 8c/i). The number of NeuN-positive cells decreased slightly after HI injury in other areas of the

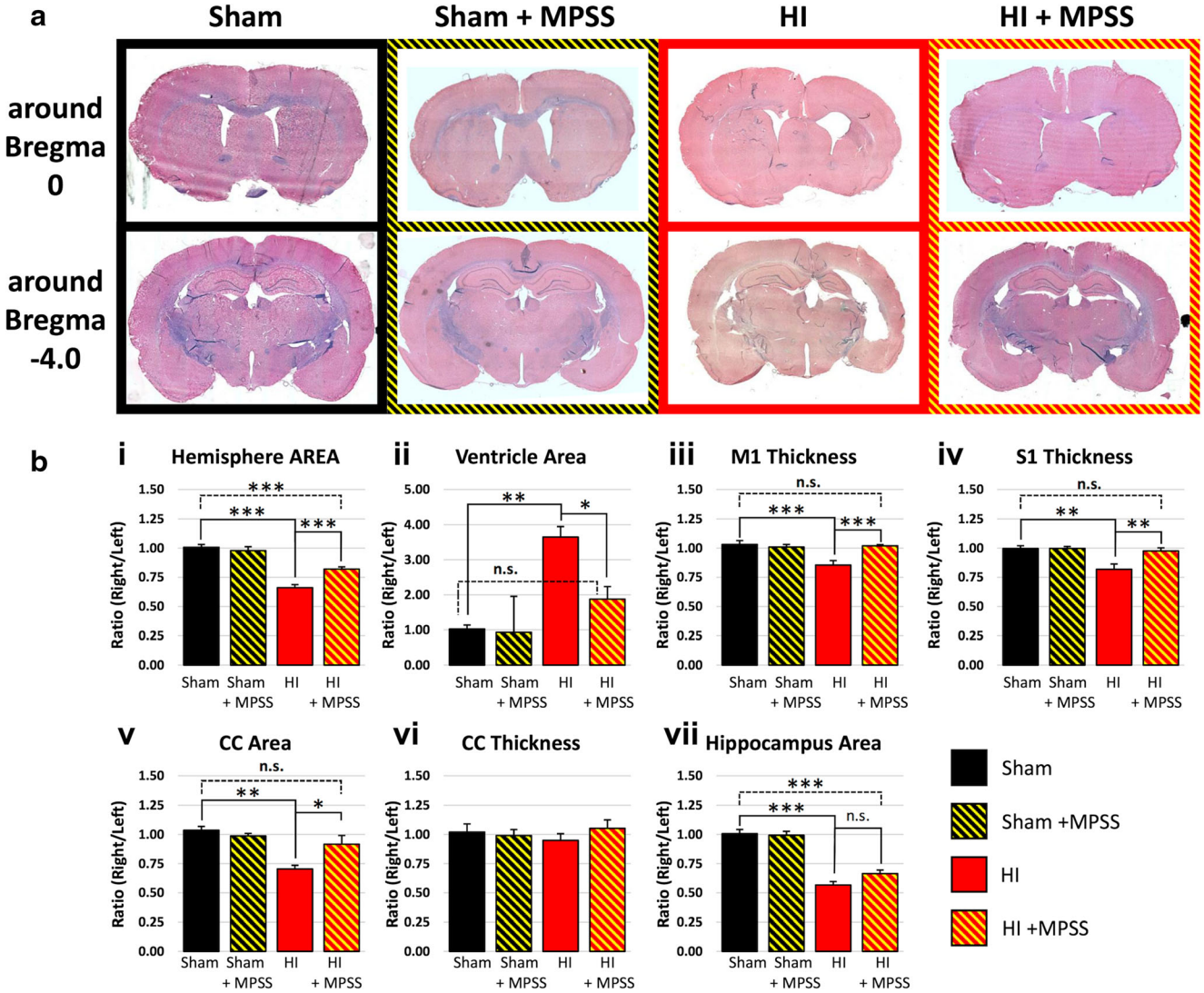

Fig. 4 Structural outcomes after HI, with or without MPSS treatment. **a** Chronic histopathological changes following HI are attenuated by P21–22 MPSS treatment. Representative images of LFB/H&E stained brain sections from Sham (Control), injured (HI), Sham-treated (Sham + MPSS) and injured treated (HI + MPSS) rats at P56 showing structural lesions. Two Bregma levels, around 0 and − 4.0 mm (respectively anterior and posterior regions), are presented. **b** Assessment of various brain structures following HI with or without P21–22 MPSS treatment. The right/left ratio of the brain hemisphere area (i), M1 (iii) and S1 (iv) thickness, corpus callosum (CC) area (v), as well as hippocampus area (vii) are decreased after HI (red bar), showing the atrophy of the right hemisphere. The right ventricle area (ii) is dramatically increased after HI, while the CC thickness (vi) does not show a significant change after injury. Delayed MPSS treatment partially restores the structural integrity (red/yellow stripes bars). Number of rats used (*n*=): 6 Sham, 7 Sham + MPSS, 10 HI and 11 HI + MPSS. Values reported are mean ± SEM. n.s. = not significant; *$p < 0.05$, **$p < 0.01$ and ***$p < 0.001$

ipsilateral hemisphere: cortex (M1 0.90 ± 0.06; S1 0.80 ± 0.10), CPu (0.66 ± 0.12) (Fig. 7a/ii, iii and iv), CA3 (0.79 ± 0.06) (Fig. 8a/iii) and thalamus (0.78 ± 0.05) (Fig. 8a/iv), when compared to sham animals for M1 (1.02 ± 0.07, $p = 0.932$), S1 (0.98 ± 0.10, $p = 0.959$), CPu (0.96 ± 0.15, $p = 0.486$), CA3 (1.03 ± 0.10, $p = 0.096$) and thalamus (1.01 ± 0.11, $p = 0.547$). After MPSS treatment, the neuronal population was not fully restored (M1 0.97 ± 0.06; S1 0.97 ± 0.10; CPu 0.94 ± 0.08; CA3 0.95 ± 0.05; thalamus 0.87 ± 0.08), when compared to untreated HI animals (M1 0.90 ± 0.06, $p = 0.981$; S1 0.80 ± 0.10, $p = 0.895$; CPu 0.66 ± 0.12, $p = 0.283$; CA3 0.79 ± 0.06, $p = 0.301$; thalamus 0.78 ± 0.05, $p = 0.978$) (Fig. 7c/i, ii and iii and Fig. 8c/ii and iii).

Delayed MPSS Treatment Attenuates Oligodendrocyte Loss in the CC

The oligodendrocyte population (Fig. 9a/ii; Supplemental Fig. 2)—empty arrowheads, Olig2+/CC1−) was significantly decreased in the ipsilateral CC after HI injury (0.53 ± 0.05) compared to sham animals (1.02 ± 0.19, $p = 0.010$). After MPSS treatment, the Olig2-positive cell

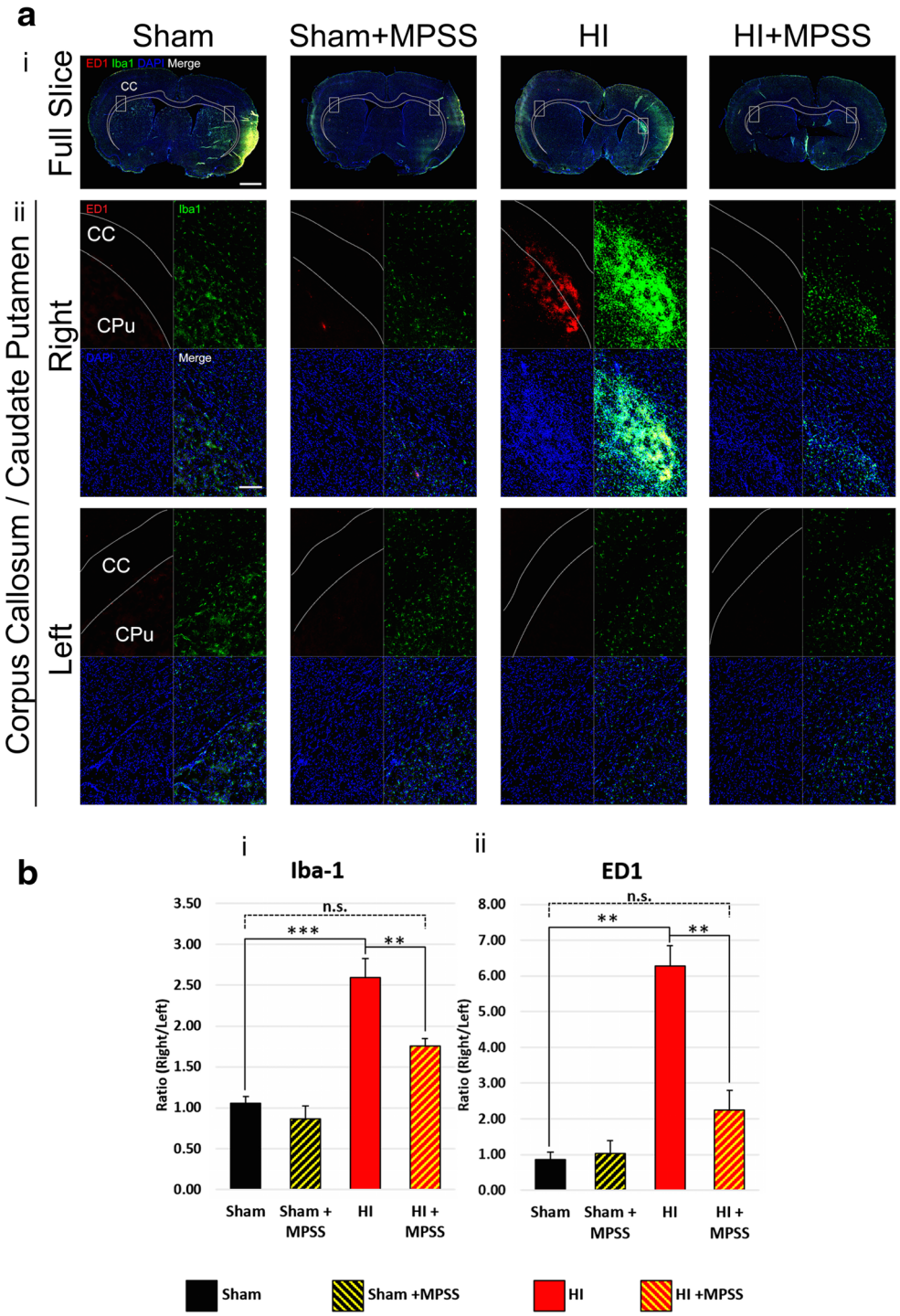

Fig. 5 MPSS treatment leads to recovery of the brain microglia/macrophages population (anterior region). **a** The double staining of Iba-1/ED1 inflammatory markers at P56 showed the inflammation state in the corpus callosum/caudate putamen (CC/CPu). Upper panels show representative pictures of whole brain slices (i) of the four experimental groups. Lower panels show a magnified view of the right (ii) and left CC/CPu: microglia Iba-1 (green), activated microglia ED1 (red), DAPI (blue) and merged colours show increased expression in the CC/CPu of the injured hemisphere. After MPSS treatment, restoration was observed. **b** Quantitative assessments confirmed the significant increase of Iba-1 (i) and ED1 (ii) markers following HI. After MPSS treatment, quantitative assessment confirmed a significant restoration of the marker levels. Scale bar is 1000 μm for whole brain slices and 200 μm for fragments. Number of rats used (*n*=): 6 Sham, 7 Sham + MPSS, 10 HI and 11 HI + MPSS. Values reported are mean ± SEM. n.s. = not significant; *$p < 0.05$, **$p < 0.01$ and ***$p < 0.001$

population was significantly restored (0.95 ± 0.08) compared to untreated HI animals (0.53 ± 0.05, $p = 0.011$) (Fig. 9b/i). The astrocyte population (Fig. 9b/ii; Supplemental Fig. 2—filled arrowheads, Olig2−/CC1+) in the ipsilateral CC of injured animals was not affected by HI injury (0.93 ± 0.08) when compared to sham animals (0.86 ± 0.18, $p = 0.999$). This population of cells also did not change in the ipsilateral CC of animals that received MPSS injections (0.91 ± 0.23) compared to untreated injured HI animals (0.93 ± 0.08, $p > 0.999$). We observed that mature oligodendrocytes (Fig. 9b/iii; Supplemental Fig. 2—yellow arrows, Olig2+/CC1+) in the CC decreased in injured animals (0.63 ± 0.06) compared to sham animals (1.00 ± 0.08, $p = 0.009$). After

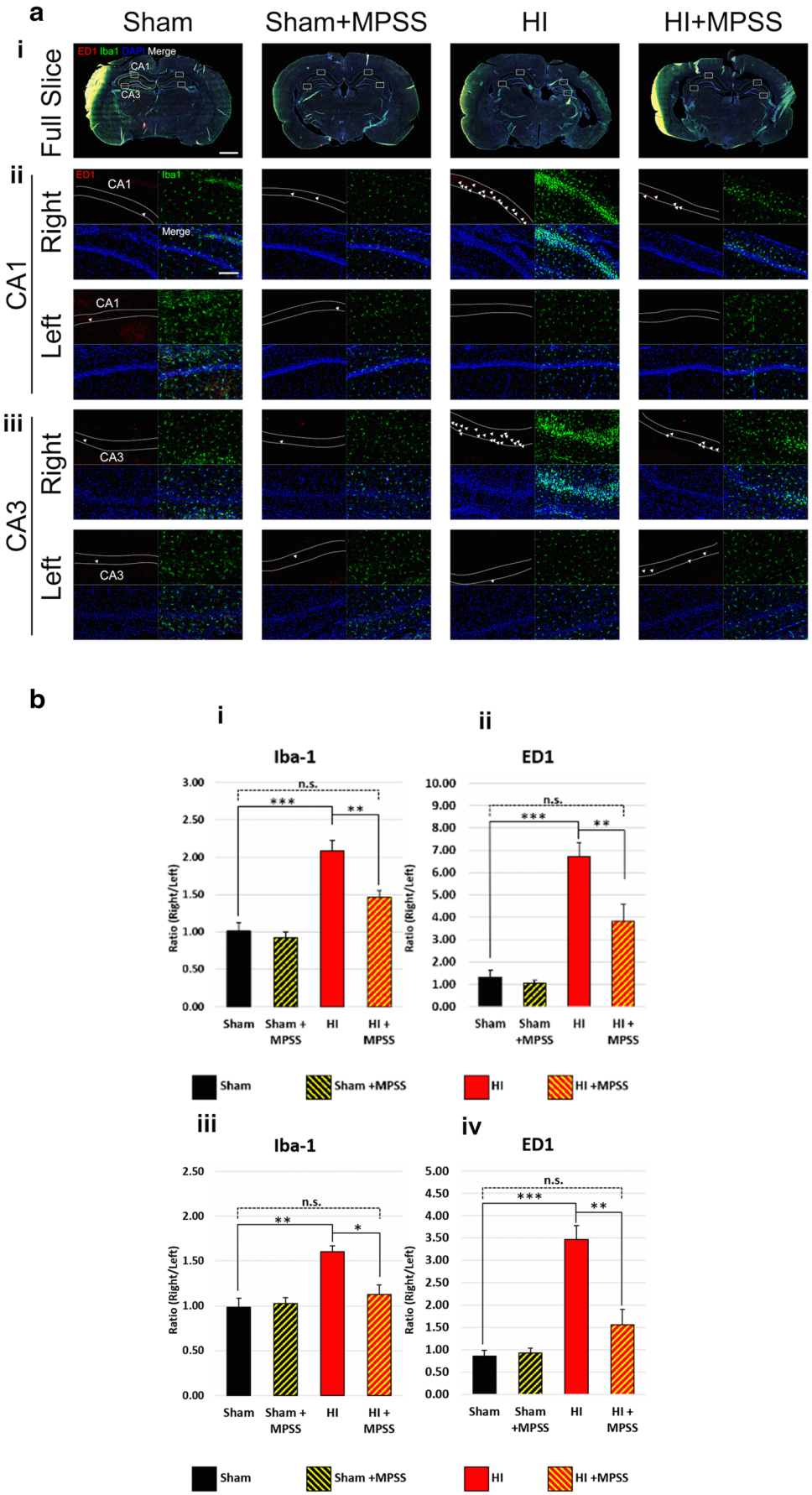

Fig. 6 MPSS treatment leads to recovery of the brain microglia/macrophages population (posterior region). **a** The double staining of Iba-1/ED1 inflammatory markers at P56 showed inflammation state of the CA1 and CA3 regions of the hippocampus. Upper panels show representative pictures of whole brain slices (i) of the four experimental groups. Lower panels show magnified view of the CA1 (ii) and CA3 (iii) hippocampus regions. The double staining microglia Iba-1 (green), activated microglia ED1 (red), DAPI (blue) and merged colours at P56 showed an expression increase in the hippocampus (ii, CA1 and iii, CA3) after HI. After MPSS treatment, a restoration was observed. **b** Quantitative assessments confirmed the increase of Iba-1 (i and iii) and ED1 (ii and iv) markers after HI in the CA1 (i-ii) and CA3 (iii-iv) areas of the hippocampus. Scale bar is 1000 μm for whole brain slices and 200 μm for fragments. Number of rats used (*n*=): 6 Sham, 7 Sham + MPSS, 10 HI and 11 HI + MPSS. Values reported are mean ± SEM. n.s. = not significant; $*p < 0.05$, $**p < 0.01$ and $***p < 0.001$

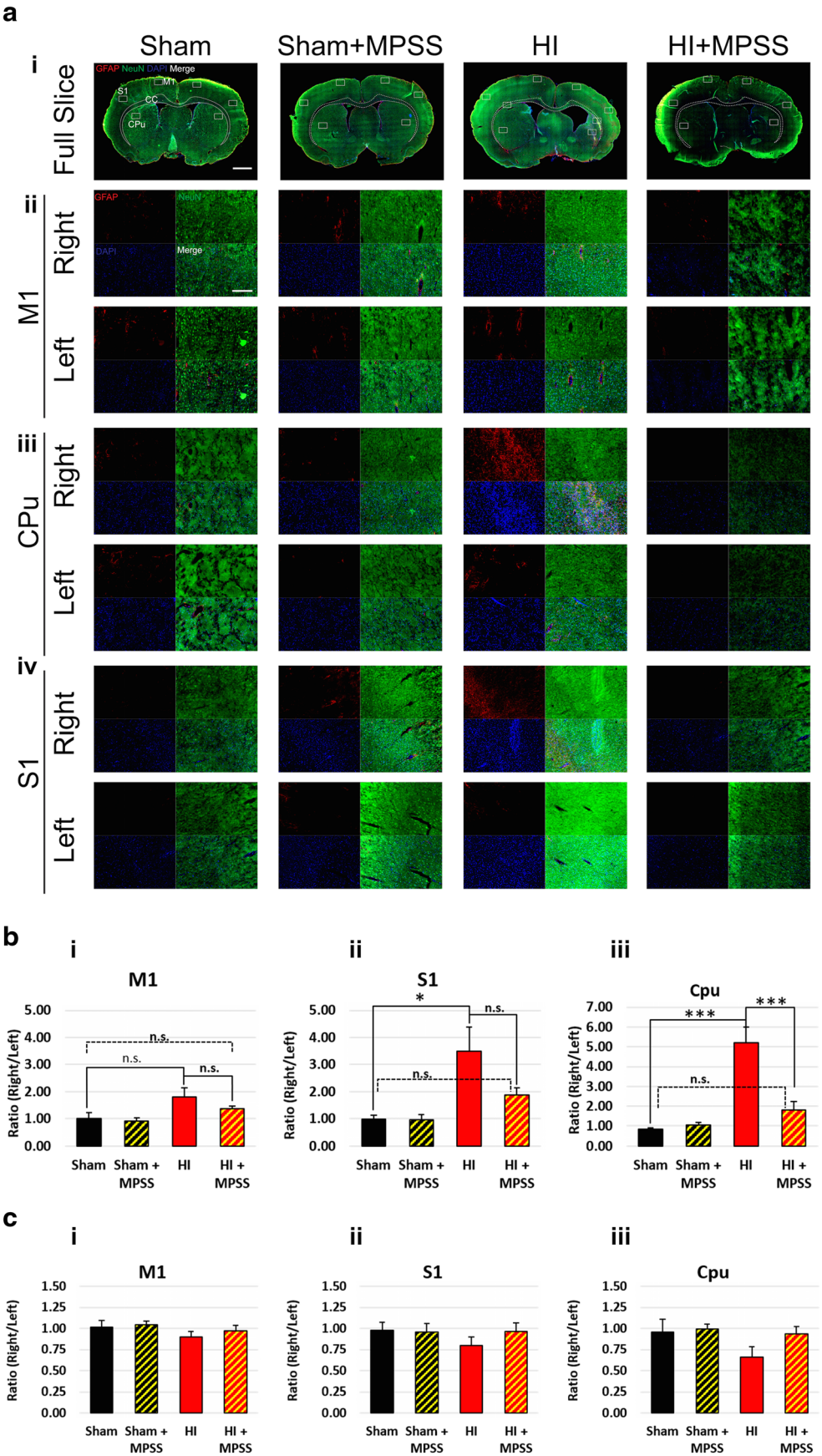

Fig. 7 MPSS treatment reduces gliosis in the Cortex (M1 and S1) and caudate but has a limited impact on the neuronal population at P56. **a** Representative pictures of the whole brain slices (i) and magnified views of GFAP (red), NeuN (green), DAPI (blue) in the M1 (ii) and S1 (iv) regions of the cortex, as well as in the CPu (iii). **b** Quantitative assessment (GFAP area measurements) demonstrated that HI triggered gliosis in the M1 and S1 cortex (i and ii respectively), as well as in the CPu (iii). After MPSS treatment, the gliosis was significantly reduced in the CPu (iii) while limited gliosis reduction was also observed in M1 and S1 areas (i and ii respectively). **c** Quantitative assessment (NeuN cell counting) in the M1 and S1 cortex (i and ii respectively), as well as in the CPu (iii), did not show significant differences. Scale bar is 1000 μm for whole brain slices and 200 μm for fragments. Number of rats used (*n*=): 6 Sham, 7 Sham + MPSS, 10 HI and 11 HI + MPSS. Values reported are mean ± SEM. n.s. = not significant; $*p < 0.05$, $**p < 0.01$ and $***p < 0.001$

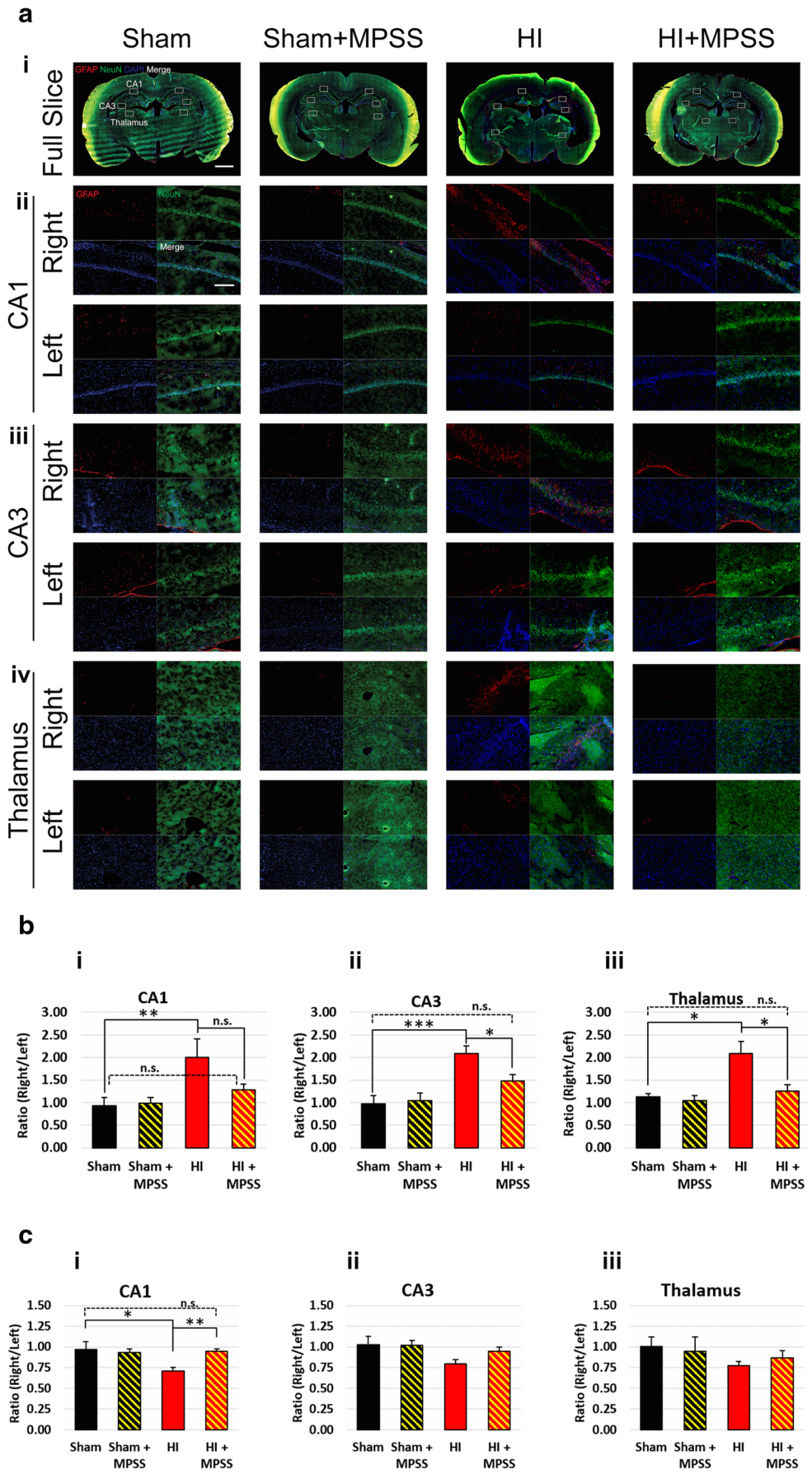
a
Sham
Sham+MPSS
HI
HI+MPSS
i
Full Slice
GFAP NeuN DAPI Merge
CA1
CA3
Thalamus
ii
CA1
Right
Left
GFAP
NeuN
DAPI
Merge
iii
CA3
Right
Left
iv
Thalamus
Right
Left
b
i
CA1
ii
CA3
iii
Thalamus
Ratio (Right/Left)
n.s.
**
***
*
Sham
Sham + MPSS
HI
HI + MPSS
c
i
CA1
ii
CA3
iii
Thalamus
Ratio (Right/Left)
n.s.
*
**
Sham
Sham + MPSS
HI
HI + MPSS

◀ **Fig. 8** MPSS treatment reduces gliosis in the hippocampus (CA1 and CA3) and thalamus at P56 but has a limited impact on the neuronal population. **a** Representative pictures of the whole brain slices (i) and magnified views of GFAP (red), NeuN (green), DAPI (blue) in the CA1 (ii) and CA3 (iii) regions of the hippocampus, as well as in the thalamus (iv). **b** Quantitative assessment (GFAP area measurements) demonstrated that HI triggered gliosis in the CA1 and CA3 hippocampus (i and ii respectively), as well as in the thalamus (iii). After MPSS treatment, the gliosis was reduced in the hippocampus and thalamus. **c** Quantitative assessment (NeuN cell counting) in the CA1 and CA3 hippocampus (i and ii respectively), as well as in the thalamus (iii), only showed significant differences in CA1. Scale bar is 1000 μm for whole brain slices and 200 μm for fragments. Number of rats used (n=): 6 Sham, 7 Sham + MPSS, 10 HI and 11 HI + MPSS. Values reported are mean ± SEM. n.s. = not significant; *$p < 0.05$, **$p < 0.01$ and ***$p < 0.001$

MPSS treatment, we observed partial restoration (0.90 ± 0.07) compared to injured animals (0.63 ± 0.06, $p = 0.037$) (Fig. 9b/iii).

Delayed MPSS Administration Results in Neurobehavioral Recovery

Behavioural tests showed persistent functional deficits in HI rats compared to Sham. The Cylinder test (Fig. 10a) baseline (P21) demonstrated a clear preference for the use of the right (unaffected) forelimb (65.68 ± 1.55), when compared to sham animals (50.72 ± 0.92, $p < 0.001$). At P56, HI animals still showed a strong preference for the right forelimb (68.57 ± 3.29), when compared to sham animals (50.78 ± 0.88,

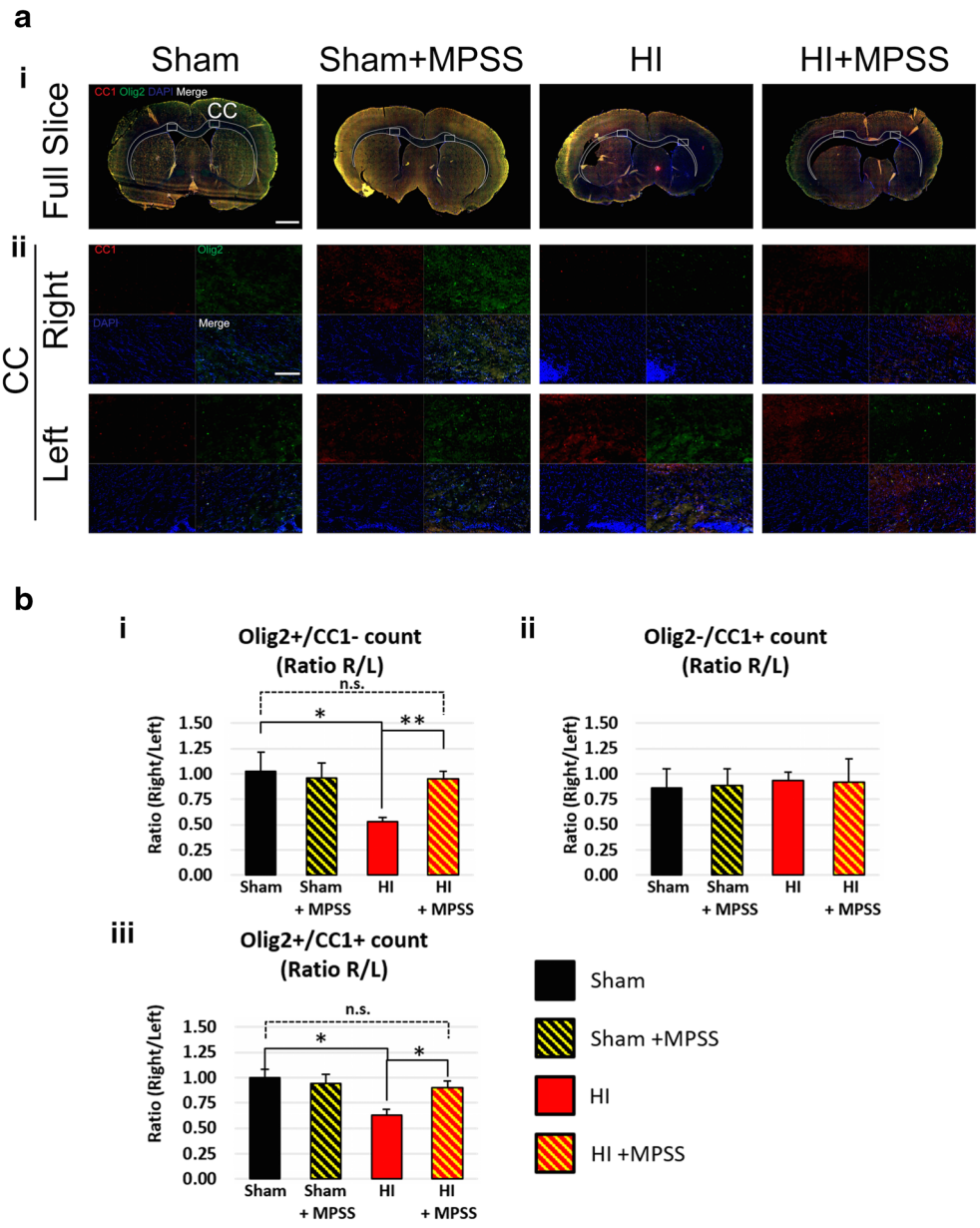

Fig. 9 MPSS treatment restores the oligodendrocyte population in the corpus callosum at P56. **a** Representative pictures of whole brain slices (i) and magnified views of CC1 (red), Olig2 (green) and DAPI (blue) in the corpus callosum (ii). CC1+/Olig2− cells are astrocytes, while CC1 −/Olig2+ cells are oligodendrocytes, and CC1+/Olig2+ are mature oligodendrocytes. A decrease in oligodendrocyte populations (including mature) is observed. After treatment, we noted a restoration of the cell number. **b** Quantitative assessment (cell counting) of oligodendrocytes (i), astrocytes (ii) and mature oligodendrocytes (iii) demonstrated a significant decrease in the oligodendrocyte population (i) including the mature subpopulation (iii). After MPSS treatment, the populations were normalised. Cell counting was performed on the Z-stack images obtained from confocal microscope that are presented in Supplemental Figure 2. Scale bar is 1000 μm for whole brain slices, and 200 μm for fragments. Number of rats used (n=): 6 Sham, 7 Sham+ MPSS, 10 HI and 11 HI+MPSS. Values reported are mean ± SEM. n.s. = not significant; *$p < 0.05$ and **$p < 0.01$

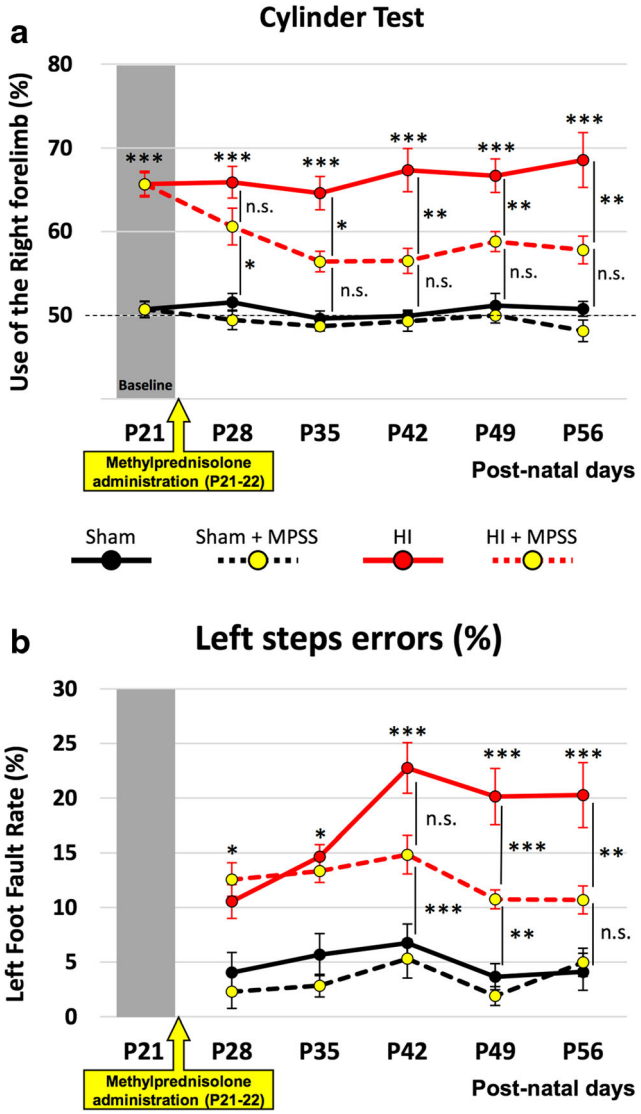

Fig. 10 MPSS treatment attenuates functional deficiencies. **a** The Cylinder test showed an increased use of the right/unaffected forelimb after HI (red line), as compared to the control (Sham—black line). After MPSS treatment, a significant recovery was observed within 2 weeks (HI + MPSS—red/yellow-dashed line). As expected, Control animals treated by MPSS did not show differences (Sham + MPSS—yellow/black-dashed line). **b** Similarly, the Ladder Rung Walking test detected an increase in the foot fault rate of the left/affected forelimb of the HI animal (red line), as compared to the control (Sham—black line). The fault rate was attenuated after MPSS treatment (HI + MPSS—red/yellow-dashed line). As expected, Control animals treated by MPSS did not show differences (Sham + MPSS—yellow/black-dashed line). NB: Postnatal day 21 (P21) is the baseline. This could not be obtained for the Ladder Rung Walking test, as the young rats, being too small, were unable to walk in a consistent manner. Number of rats used (n=): 6 Sham, 7 Sham + MPSS, 10 HI and 11 HI + MPSS. Values reported are mean ± SEM. n.s. = not significant; *$p < 0.05$, **$p < 0.01$, and ***$p < 0.001$

$p < 0.001$). At P56, MPSS-treated animals showed significant improvements (57.80 ± 1.66) compared to untreated rats (68.57 ± 3.29, $p < 0.001$). The Ladder Rung Walking test (Fig. 10b) indicated that foot fault rates for the HI group increased at the start of the testing period (10.55 ± 1.55) compared to sham animals (4.04 ± 1.83, $p < 0.05$). At P56, HI animals had an increased foot fault rate (20.26 ± 2.98) when compared to sham animals (4.10 ± 1.70, $p < 0.001$). Treated rats showed a significant improvement in the foot fault rate (10.69 ± 1.58) at P56 when compared to untreated animals (20.26 ± 2.98, $p < 0.01$). MPSS treatment gradually improved behaviour outcomes and reached statistical significance on the Cylinder test at P35, while significant improvements on the Ladder Rung Walking test were noted at P49 (2 and 4 weeks after injections, respectively).

Discussion

In the present study, we focused on the chronic inflammation that persists during the secondary and tertiary phases of injury following perinatal stroke. In our neonatal HI model, we demonstrated persistent expression of pro-inflammatory cytokines, brain structural impairments and motor deficiencies. We showed that, following treatment with MPSS, the levels of pro-inflammatory cytokines were significantly reduced resulting in the attenuation of brain lesions and motor function improvement. The delayed MPSS treatment improved microglial, astroglial and oligodendrocyte populations but only partially restored neuronal populations. As the inflammatory process exacerbates neonatal brain injuries [8, 9, 58, 59], a treatment for persistent inflammation is therefore clinically pertinent.

Chronic Inflammation Following Perinatal Stroke

There is a growing body of research that demonstrates persistent inflammation during the tertiary phase of brain damage [9, 13]. In line with this work, we demonstrated that inflammation persists long after the initial HI injury. Our RT-qPCR data demonstrating elevations in IL-18, CCL3 and CCL5 after HI injury are in agreement with prior research [21, 23]. Of note, elevated levels of IL-18 in the pup brain up to P21 suggest a central role of IL-18 in neonatal injury [22, 23]. We also observed an elevation of TNFα; however, this was not statistically significant. The change in TNFα may indicate an early transient increase, as previously shown by other groups [21, 60]. Our results therefore confirm an ongoing inflammatory process that continues beyond the initial acute injury into the chronic phase of perinatal stroke, likely resulting in further injury.

Treatment of Chronic Inflammation

Managing inflammation is a promising therapeutic strategy to attenuate ongoing brain injury, which should in turn improve outcomes following perinatal stroke. Previously,

corticosteroids have been injected in animals prior to injury or acutely after injury in models of perinatal stroke [26] or adult transient cerebral ischemia [29, 46] to reduce the extent of neuroinflammation. For example, Ikeda et al. previously showed that dexamethasone pre-treatment 4 h before HI, combined with LPS on P7 rat pups, significantly prevented brain structure reductions as well as impairments in learning and memory tasks [61].

While treatment before the HI insult is not clinically relevant, treatment within the first hours of injury is also unlikely as clinical diagnosis may not be accurate at this time. Therefore, delayed treatment is more feasible in the case of perinatal stroke. Thus, we investigated the potential of an anti-inflammatory treatment in the tertiary stage of injury to improve functional outcomes. In contrast to past work, our study utilized delayed MPSS administration and was able to demonstrate significant decreases in pro-inflammatory cytokines and brain structural impairments, while also improving motor function.

Using MPSS administered at P21, we observed significant decreases in the cytokine IL-18 as well as chemokines CCL3 and CCL5 in the injured ipsilateral hemisphere. Further, the microglia activation (Iba-1 and ED1 immunostaining) and gliosis (GFAP immunostaining) in the injured side of the brain were reduced after delayed MPSS treatment. It has been previously reported that expression of CCL3 and CCL5 precedes microglia and macrophage activation after HI injury [21]. Microglia, as well as astrocytes, oligodendrocytes and immune cells, may be sources of cytokines and chemokines in perinatal stroke [62–64]. Since we observed elevated cytokine gene expression in the injured brain hemisphere (2 and 3 weeks post HI), we investigated markers of cell populations at delayed timepoints (i.e. 7 weeks after injury). We have found that perinatal stroke induced microglia activation (Iba-1 and ED1 immunostaining) and gliosis (GFAP immunostaining) in the injured side of the brain, which was reduced after delayed MPSS treatment. Furthermore, the observed decreases in neuronal and oligodendrocyte populations (including mature oligodendrocytes) after HI [42, 55] were restored following delayed MPSS injection. Treatment with MPSS during the tertiary phase following perinatal stroke was shown to reduce gliosis, microglial activation and oligodendrocyte loss in the injured brain hemisphere.

Following HI injury, our behavioural testing revealed motor impairments such as a preference for the use of the unaffected forelimb. MPSS treatment significantly improved motor function, most likely by reducing inflammation. Okada et al. have shown that functional recovery improved after the signalling mitigation of cytokines such as IL-6 [65]. Furthermore, past work has demonstrated that neuroinflammation results in white matter injury and hypomyelination, leading to sensorimotor deficits [66, 67]. We have shown here that the attenuation of inflammation contributes to partial restoration of the oligodendrocyte population. The subsequent restoration of white matter integrity could therefore contribute to motor function improvement, as was observed in our recent publication describing a cell-based treatment leading to motor recovery in a perinatal stroke mouse model [42].

Lymphocytes and macrophages are also major components of inflammation processes. While it has been proposed that glucocorticoids can support the survival of T cells [68] and lead to an increase of the regulatory T cells counts [69], other researchers have suggested that regulatory T cell populations do not significantly increase [70]. Interestingly, we have previously shown that MPSS does not affect peripheral white blood cells in degenerative cervical myelopathy [50]; however, further studies are required to determine the precise role played by T cells following treatment of HI with MPSS.

Translation Potential of Methylprednisolone

Our findings show that MPSS has strong translational potential as a treatment in the chronic phase of injury. To date, most research has focused on early interventions using corticosteroids. However, adverse outcomes were reported following dexamethasone or betamethasone treatment in newborns, leading to a higher risk of developing CP and impaired memory [71–73]. Negative effects of glucocorticoids in children have been reported [74], perhaps due to concentrations that were too high or administered for too long. Animal studies have shown that dexamethasone pre-treatment protected 1 and 2 weeks old rat pups from HI injury but did not have an effect on 1 month old animals [75]. As glucocorticoids may decrease systemic resistance to bacterial infections [76], a shorter treatment course may be preferable.

Interestingly, our study demonstrates positive effects of MPSS treatment at 3 weeks, a critical window for CP diagnosis. While this time frame is clinically relevant, MPSS may produce beneficial effects if also administered at earlier time points [24, 43, 46]. In addition, MPSS has been found to be as effective as the widely used dexamethasone, while triggering fewer side effects in the case of preterm infants [77]. Interestingly, it was recently reported that 5 days of intravenous high-dose MPSS administration (30 mg/kg/day) induced complete recovery in an 11-month-old child with subacute stroke in the right occipital lobe and bilateral cerebellar hemorrhagic infarcts due to osmotic demyelination syndrome. After this short treatment, follow-ups at 3 months and 2 years old showed normal development [36].

The long-term outcomes of MPSS treatment have not been fully assessed in neonatal HI. While some studies suggest negative effects [74, 78], others have reported beneficial effects [77, 79]. In the present study, we did not observe significant long-term adverse outcomes after assessing the animals up to P56, which roughly corresponds to 20+ years in humans [39]. A recent systematic review did not indicate major side

effects [76]; however, further investigation is needed to clarify this issue.

Delayed MPSS administration, via I.V. injections, holds great promise for the treatment of chronic inflammation and injury. Our study represents an important step in bridging the gap between experimental and clinical end points and offers rapid translational potential.

Conclusion

Our study demonstrates that persistent brain inflammation is a key mechanism of injury in the developing brain resulting in functional deficits. We showed that the delayed administration of MPSS modulated this chronic inflammation, leading to significant recovery at multiple levels (i.e. structural, cellular, functional). Future studies are necessary to further decipher the underlying mechanisms of MPSS effects and to address crucial questions with regard to therapeutic strategies (improved dosage, frequency, timing). This research holds high translational value and demonstrates that MPSS is useful during the delayed post-injury period.

Funding Information This study was funded by the Kids Brain Health Network and Ontario Brain Institute.

Compliance with Ethical Standards

Experimental procedures, animal use and care were approved by the Animal Care Committee at the University Health Network in accordance with the policies and procedures outlined by the Canadian Council of Animal Care.

Conflict of Interest The authors declare that they have no conflict of interest.

Ethical Approval All applicable international, national and/or institutional guidelines for the care and use of animals were followed. Experimental procedures, animal use and care were approved by the Animal Care Committee at the University Health Network in accordance with the policies and procedures outlined by the Canadian Council of Animal Care.

References

1. de Veber GA, Kirton A, Booth FA, Yager JY, Wirrell EC, Wood E, et al. Epidemiology and outcomes of arterial ischemic stroke in children: the Canadian Pediatric Ischemic Stroke Registry. Pediatr Neurol. 2017;69:58–70. https://doi.org/10.1016/j.pediatrneurol.2017.01.016.
2. Giudice C, Rogers EE, Johnson BC, Glass HC, Shapiro KA. Neuroanatomical correlates of sensory deficits in children with neonatal arterial ischemic stroke. Dev Med Child Neurol. 2018. https://doi.org/10.1111/dmcn.14101.
3. Nelson KB. Perinatal ischemic stroke. Stroke. 2007;38(2 Suppl):742–5. https://doi.org/10.1161/01.STR.0000247921.97794.5e.
4. Wagenaar N, Martinez-Biarge M, van der Aa NE, van Haastert IC, Groenendaal F, Benders M, et al. Neurodevelopment after perinatal arterial ischemic stroke. Pediatrics. 2018;142(3). https://doi.org/10.1542/peds.2017-4164.
5. Kirton A, Deveber G. Life after perinatal stroke. Stroke. 2013;44(11):3265–71. https://doi.org/10.1161/strokeaha.113.000739.
6. Mineyko A, Kirton A. The black box of perinatal ischemic stroke pathogenesis. J Child Neurol. 2011;26(9):1154–62. https://doi.org/10.1177/0883073811408312.
7. Hagberg H, David Edwards A, Groenendaal F. Perinatal brain damage: the term infant. Neurobiol Dis. 2016;92(Pt A):102–12. https://doi.org/10.1016/j.nbd.2015.09.011.
8. Van Steenwinckel J, Schang AL, Sigaut S, Chhor V, Degos V, Hagberg H, et al. Brain damage of the preterm infant: new insights into the role of inflammation. Biochem Soc Trans. 2014;42(2):557–63. https://doi.org/10.1042/bst20130284.
9. Fleiss B, Gressens P. Tertiary mechanisms of brain damage: a new hope for treatment of cerebral palsy? Lancet Neurol. 2012;11(6):556–66. https://doi.org/10.1016/s1474-4422(12)70058-3.
10. Ek CJ, D'Angelo B, Baburamani AA, Lehner C, Leverin AL, Smith PL, et al. Brain barrier properties and cerebral blood flow in neonatal mice exposed to cerebral hypoxia-ischemia. J Cereb Blood Flow Metab. 2015;35(5):818–27. https://doi.org/10.1038/jcbfm.2014.255.
11. Lee WLA, Michael-Titus AT, Shah DK. Hypoxic-ischaemic encephalopathy and the blood-brain barrier in neonates. Dev Neurosci. 2017;39(1–4):49–58. https://doi.org/10.1159/000467392.
12. Rumajogee P, Bregman T, Miller SP, Yager JY, Fehlings MG. Rodent hypoxia-ischemia models for cerebral palsy research: a systematic review. Front Neurol. 2016;7:57. https://doi.org/10.3389/fneur.2016.00057.
13. Hagberg H, Mallard C, Ferriero DM, Vannucci SJ, Levison SW, Vexler ZS, et al. The role of inflammation in perinatal brain injury. Nat Rev Neurol. 2015;11(4):192–208. https://doi.org/10.1038/nrneurol.2015.13.
14. Back SA. White matter injury in the preterm infant: pathology and mechanisms. Acta Neuropathol. 2017;134(3):331–49. https://doi.org/10.1007/s00401-017-1718-6.
15. Fern RF, Matute C, Stys PK. White matter injury: ischemic and nonischemic. Glia. 2014;62(11):1780–9. https://doi.org/10.1002/glia.22722.
16. Liu F, McCullough LD. Inflammatory responses in hypoxic ischemic encephalopathy. Acta Pharmacol Sin. 2013;34(9):1121–30. https://doi.org/10.1038/aps.2013.89.
17. Favrais G, van de Looij Y, Fleiss B, Ramanantsoa N, Bonnin P, Stoltenburg-Didinger G, et al. Systemic inflammation disrupts the developmental program of white matter. Ann Neurol. 2011;70(4):550–65. https://doi.org/10.1002/ana.22489.
18. Ramaswamy V, Miller SP, Barkovich AJ, Partridge JC, Ferriero DM. Perinatal stroke in term infants with neonatal encephalopathy. Neurology. 2004;62(11):2088–91. https://doi.org/10.1212/01.WNL.0000129909.77753.C4.
19. Chalak LF, Sanchez PJ, Adams-Huet B, Laptook AR, Heyne RJ, Rosenfeld CR. Biomarkers for severity of neonatal hypoxic-ischemic encephalopathy and outcomes in newborns receiving hypothermia therapy. J Pediatr. 2014;164(3):468–74.e1. https://doi.org/10.1016/j.jpeds.2013.10.067.
20. Bhalala US, Koehler RC, Kannan S. Neuroinflammation and neuroimmune dysregulation after acute hypoxic-ischemic injury of developing brain. Front Pediatr. 2014;2:144. https://doi.org/10.3389/fped.2014.00144.
21. Bona E, Andersson A-L, Blomgren K, Gilland E, Puka-Sundvall M, Gustafson K, et al. Chemokine and inflammatory cell response

to hypoxia-ischemia in immature rats. Pediatr Res. 1999;45:500. https://doi.org/10.1203/00006450-199904010-00008.
22. Hedtjarn M, Mallard C, Arvidsson P, Hagberg H. White matter injury in the immature brain: role of interleukin-18. Neurosci Lett. 2005;373(1):16–20. https://doi.org/10.1016/j.neulet.2004.09.062.
23. Hedtjarn M, Leverin AL, Eriksson K, Blomgren K, Mallard C, Hagberg H. Interleukin-18 involvement in hypoxic-ischemic brain injury. J Neurosci. 2002;22(14):5910–9.
24. Daneyemez M, Kurt E, Cosar A, Yuce E, Ide T. Methylprednisolone and vitamin E therapy in perinatal hypoxic-ischemic brain damage in rats. Neuroscience. 1999;92(2):693–7.
25. Gonzalez-Rodriguez PJ, Li Y, Martinez F, Zhang L. Dexamethasone protects neonatal hypoxic-ischemic brain injury via L-PGDS-dependent PGD2-DP1-pERK signaling pathway. PLoS One. 2014;9(12):e114470. https://doi.org/10.1371/journal.pone.0114470.
26. Harding B, Conception K, Li Y, Zhang L. Glucocorticoids protect neonatal rat brain in model of hypoxic-ischemic encephalopathy (HIE). Int J Mol Sci. 2016;18(1). https://doi.org/10.3390/ijms18010017.
27. Concepcion KR, Zhang L. Corticosteroids and perinatal hypoxic-ischemic brain injury. Drug Discov Today. 2018. https://doi.org/10.1016/j.drudis.2018.05.019.
28. Cheng S, Gao W, Xu X, Fan H, Wu Y, Li F, et al. Methylprednisolone sodium succinate reduces BBB disruption and inflammation in a model mouse of intracranial haemorrhage. Brain Res Bull. 2016;127:226–33. https://doi.org/10.1016/j.brainresbull.2016.10.007.
29. Kim JS, Chopp M, Gautam SC. High dose methylprednisolone therapy reduces expression of JE/MCP-1 mRNA and macrophage accumulation in the ischemic rat brain. J Neurol Sci. 1995;128(1):28–35.
30. Hall ED. Methylprednisolone for the treatment of patients with acute spinal cord injuries: a propensity score-matched cohort study from a Canadian Multi-Center Spinal Cord Injury Registry. J Neurotrauma. 2016;33(10):972–4. https://doi.org/10.1089/neu.2016.4473.
31. Cooper SD, Felkins K, Baker TE, Hale TW. Transfer of methylprednisolone into breast milk in a mother with multiple sclerosis. J Hum Lact. 2015;31(2):237–9. https://doi.org/10.1177/0890334415570970.
32. Fehlings MG, Wilson JR, Harrop JS, Kwon BK, Tetreault LA, Arnold PM, et al. Efficacy and safety of methylprednisolone sodium succinate in acute spinal cord injury: a systematic review. Glob Spine J. 2017;7(3 Suppl):116S–37S. https://doi.org/10.1177/2192568217706366.
33. Fernandes Moca Trevisani V, Castro AA, Ferreira Neves Neto J, Atallah AN. Cyclophosphamide versus methylprednisolone for treating neuropsychiatric involvement in systemic lupus erythematosus. Cochrane Database Syst Rev. 2013;(2):CD002265. https://doi.org/10.1002/14651858.CD002265.pub3.
34. Hall ED. The neuroprotective pharmacology of methylprednisolone. J Neurosurg. 1992;76(1):13–22. https://doi.org/10.3171/jns.1992.76.1.0013.
35. Oudega M, Vargas CG, Weber AB, Kleitman N, Bunge MB. Long-term effects of methylprednisolone following transection of adult rat spinal cord. Eur J Neurosci. 1999;11(7):2453–64.
36. Bansal LR. Therapeutic effect of steroids in osmotic demyelination of infancy. Child Neurol Open. 2018;5:2329048x18770576. https://doi.org/10.1177/2329048x18770576.
37. Graham HK, Rosenbaum P, Paneth N, Dan B, Lin JP, Damiano DL, et al. Cerebral palsy. Nat Rev Dis Prim. 2016;2:15082. https://doi.org/10.1038/nrdp.2015.82.
38. Hubermann L, Boychuck Z, Shevell M, Majnemer A. Age at referral of children for initial diagnosis of cerebral palsy and rehabilitation: current practices. J Child Neurol. 2016;31(3):364–9. https://doi.org/10.1177/0883073815596610.
39. Semple BD, Blomgren K, Gimlin K, Ferriero DM, Noble-Haeusslein LJ. Brain development in rodents and humans: Identifying benchmarks of maturation and vulnerability to injury across species. Prog Neurobiol. 2013:106, 1–7, 16. https://doi.org/10.1016/j.pneurobio.2013.04.001.
40. Rice JE 3rd, Vannucci RC, Brierley JB. The influence of immaturity on hypoxic-ischemic brain damage in the rat. Ann Neurol. 1981;9(2):131–41. https://doi.org/10.1002/ana.410090206.
41. Vannucci RC, Vannucci SJ. Perinatal hypoxic-ischemic brain damage: evolution of an animal model. Dev Neurosci. 2005;27(2–4):81–6. https://doi.org/10.1159/000085978.
42. Rumajogee P, Altamentova S, Li L, Li J, Wang J, Kuurstra A, et al. Exogenous neural precursor cell transplantation results in structural and functional recovery in a hypoxic-ischemic hemiplegic mouse model. eNeuro. 2018;5(5). https://doi.org/10.1523/eneuro.0369-18.2018.
43. Kalayci O, Cataltepe S, Cataltepe O. The effect of bolus methylprednisolone in prevention of brain edema in hypoxic ischemic brain injury: an experimental study in 7-day-old rat pups. Brain Res. 1992;569(1):112–6.
44. Yu Y, Matsuyama Y, Nakashima S, Yanase M, Kiuchi K, Ishiguro N. Effects of MPSS and a potent iNOS inhibitor on traumatic spinal cord injury. Neuroreport. 2004;15(13):2103–7.
45. Braughler JM, Hall ED. Effects of multi-dose methylprednisolone sodium succinate administration on injured cat spinal cord neurofilament degradation and energy metabolism. J Neurosurg. 1984;61(2):290–5. https://doi.org/10.3171/jns.1984.61.2.0290.
46. Jing Y, Hou Y, Song Y, Yin J. Methylprednisolone improves the survival of new neurons following transient cerebral ischemia in rats. Acta Neurobiol Exp. 2012;72(3):240–52.
47. Braughler JM, Hall ED. Correlation of methylprednisolone levels in cat spinal cord with its effects on (Na+ + K+)-ATPase, lipid peroxidation, and alpha motor neuron function. J Neurosurg. 1982;56(6):838–44. https://doi.org/10.3171/jns.1982.56.6.0838.
48. Hall ED, Braughler JM, McCall JM. Antioxidant effects in brain and spinal cord injury. J Neurotrauma. 1992;9(Suppl 1):S165–72.
49. Hall ED, Wolf DL, Braughler JM. Effects of a single large dose of methylprednisolone sodium succinate on experimental posttraumatic spinal cord ischemia. Dose-response and time-action analysis. J Neurosurg. 1984;61(1):124–30. https://doi.org/10.3171/jns.1984.61.1.0124.
50. Vidal PM, Ulndreaj A, Badner A, Hong J, Fehlings MG. Methylprednisolone treatment enhances early recovery following surgical decompression for degenerative cervical myelopathy without compromise to the systemic immune system. J Neuroinflammation. 2018;15(1):222. https://doi.org/10.1186/s12974-018-1257-7.
51. Forgione N, Chamankhah M, Fehlings MG. A mouse model of bilateral cervical contusion-compression spinal cord injury. J Neurotrauma. 2017;34(6):1227–39. https://doi.org/10.1089/neu.2016.4708.
52. Cai J, Kang Z, Liu WW, Luo X, Qiang S, Zhang JH, et al. Hydrogen therapy reduces apoptosis in neonatal hypoxia-ischemia rat model. Neurosci Lett. 2008;441(2):167–72. https://doi.org/10.1016/j.neulet.2008.05.077.
53. Ruff CA, Ye H, Legasto JM, Stribbell NA, Wang J, Zhang L, et al. Effects of adult neural precursor-derived myelination on axonal function in the perinatal congenitally dysmyelinated brain: optimizing time of intervention, developing accurate prediction models, and enhancing performance. J Neurosci. 2013;33(29):11899–915. https://doi.org/10.1523/JNEUROSCI.1131-13.2013.
54. Karimi-Abdolrezaee S, Eftekharpour E, Wang J, Schut D, Fehlings MG. Synergistic effects of transplanted adult neural stem/progenitor cells, chondroitinase, and growth factors promote

functional repair and plasticity of the chronically injured spinal cord. J Neurosci. 2010;30(5):1657–76. https://doi.org/10.1523/JNEUROSCI.3111-09.2010.
55. Beldick SR, Hong J, Altamentova S, Khazaei M, Hundal A, Zavvarian MM, et al. Severe-combined immunodeficient rats can be used to generate a model of perinatal hypoxic-ischemic brain injury to facilitate studies of engrafted human neural stem cells. PLoS One. 2018;13(11):e0208105. https://doi.org/10.1371/journal.pone.0208105.
56. Goto N. Discriminative staining methods for the nervous system: luxol fast blue–periodic acid-Schiff–hematoxylin triple stain and subsidiary staining methods. Stain Technol. 1987;62(5):305–15.
57. Metz GA, Whishaw IQ. Cortical and subcortical lesions impair skilled walking in the ladder rung walking test: a new task to evaluate fore- and hindlimb stepping, placing, and co-ordination. J Neurosci Methods. 2002;115(2):169–79.
58. Fleiss B, Tann CJ, Degos V, Sigaut S, Van Steenwinckel J, Schang AL, et al. Inflammation-induced sensitization of the brain in term infants. Dev Med Child Neurol. 2015;57(Suppl 3):17–28. https://doi.org/10.1111/dmcn.12723.
59. Moretti R, Pansiot J, Bettati D, Strazielle N, Ghersi-Egea JF, Damante G, et al. Blood-brain barrier dysfunction in disorders of the developing brain. Front Neurosci. 2015;9:40. https://doi.org/10.3389/fnins.2015.00040.
60. Shrivastava K, Llovera G, Recasens M, Chertoff M, Gimenez-Llort L, Gonzalez B, et al. Temporal expression of cytokines and signal transducer and activator of transcription factor 3 activation after neonatal hypoxia/ischemia in mice. Dev Neurosci. 2013;35(2–3):212–25. https://doi.org/10.1159/000348432.
61. Ikeda T, Mishima K, Aoo N, Liu AX, Egashira N, Iwasaki K, et al. Dexamethasone prevents long-lasting learning impairment following a combination of lipopolysaccharide and hypoxia-ischemia in neonatal rats. Am J Obstet Gynecol. 2005;192(3):719–26. https://doi.org/10.1016/j.ajog.2004.12.048.
62. Benveniste EN. Inflammatory cytokines within the central nervous system: sources, function, and mechanism of action. Am J Phys. 1992;263(1 Pt 1):C1–16. https://doi.org/10.1152/ajpcell.1992.263.1.C1.
63. Benveniste EN. Cytokines: influence on glial cell gene expression and function. Chem Immunol. 1992;52:106–53.
64. Ramesh G, MacLean AG, Philipp MT. Cytokines and chemokines at the crossroads of neuroinflammation, neurodegeneration, and neuropathic pain. Mediat Inflamm. 2013;2013:480739. https://doi.org/10.1155/2013/480739.
65. Okada S, Nakamura M, Mikami Y, Shimazaki T, Mihara M, Ohsugi Y, et al. Blockade of interleukin-6 receptor suppresses reactive astrogliosis and ameliorates functional recovery in experimental spinal cord injury. J Neurosci Res. 2004;76(2):265–76. https://doi.org/10.1002/jnr.20044.
66. Donnelly DJ, Popovich PG. Inflammation and its role in neuroprotection, axonal regeneration and functional recovery after spinal cord injury. Exp Neurol. 2008;209(2):378–88. https://doi.org/10.1016/j.expneurol.2007.06.009.
67. Taib T, Leconte C, Van Steenwinckel J, Cho AH, Palmier B, Torsello E, et al. Neuroinflammation, myelin and behavior: temporal patterns following mild traumatic brain injury in mice. PLoS One. 2017;12(9):e0184811. https://doi.org/10.1371/journal.pone.0184811.
68. Ashwell JD, Lu FW, Vacchio MS. Glucocorticoids in T cell development and function*. Annu Rev Immunol. 2000;18:309–45. https://doi.org/10.1146/annurev.immunol.18.1.309.
69. Mathian A, Jouenne R, Chader D, Cohen-Aubart F, Haroche J, Fadlallah J, et al. Regulatory T cell responses to high-dose methylprednisolone in active systemic lupus Erythematosus. PLoS One. 2015;10(12):e0143689. https://doi.org/10.1371/journal.pone.0143689.
70. Sbiera S, Dexneit T, Reichardt SD, Michel KD, van den Brandt J, Schmull S, et al. Influence of short-term glucocorticoid therapy on regulatory T cells in vivo. PLoS One. 2011;6(9):e24345. https://doi.org/10.1371/journal.pone.0024345.
71. Jobe AH. Glucocorticoids in perinatal medicine: misguided rockets? J Pediatr. 2000;137(1):1–3. https://doi.org/10.1067/mpd.2000.107801.
72. Baud O, Sola A. Corticosteroids in perinatal medicine: how to improve outcomes without affecting the developing brain? Semin Fetal Neonatal Med. 2007;12(4):273–9. https://doi.org/10.1016/j.siny.2007.01.025.
73. Bennet L, Davidson JO, Koome M, Gunn AJ. Glucocorticoids and preterm hypoxic-ischemic brain injury: the good and the bad. J Pregnancy. 2012;2012:751694. https://doi.org/10.1155/2012/751694.
74. Damsted SK, Born AP, Paulson OB, Uldall P. Exogenous glucocorticoids and adverse cerebral effects in children. Eur J Paediatr Neurol. 2011;15(6):465–77. https://doi.org/10.1016/j.ejpn.2011.05.002.
75. Tuor UI, Chumas PD, Del Bigio MR. Prevention of hypoxic-ischemic damage with dexamethasone is dependent on age and not influenced by fasting. Exp Neurol. 1995;132(1):116–22. https://doi.org/10.1016/0014-4886(95)90065-9.
76. Aljebab F, Choonara I, Conroy S. Systematic review of the toxicity of short-course oral corticosteroids in children. Arch Dis Child. 2016;101(4):365–70. https://doi.org/10.1136/archdischild-2015-309522.
77. Baud O. Postnatal steroid treatment and brain development. Arch Dis Child Fetal Neonatal Ed. 2004;89(2):F96–100.
78. O'Shea TM, Doyle LW. Perinatal glucocorticoid therapy and neurodevelopmental outcome: an epidemiologic perspective. Semin Neonatol. 2001;6(4):293–307. https://doi.org/10.1053/siny.2001.0065.
79. Malaeb SN, Stonestreet BS. Steroids and injury to the developing brain: net harm or net benefit? Clin Perinatol. 2014;41(1):191–208. https://doi.org/10.1016/j.clp.2013.09.006.